AD-A088 602 PURDUE UNIV HAMMOND IN F/G 20/4
QUASISTEADY VISCOUS FLOWS.(U)
JUL 80 P GORDON N00014-78-C-0308
UNCLASSIFIED NL

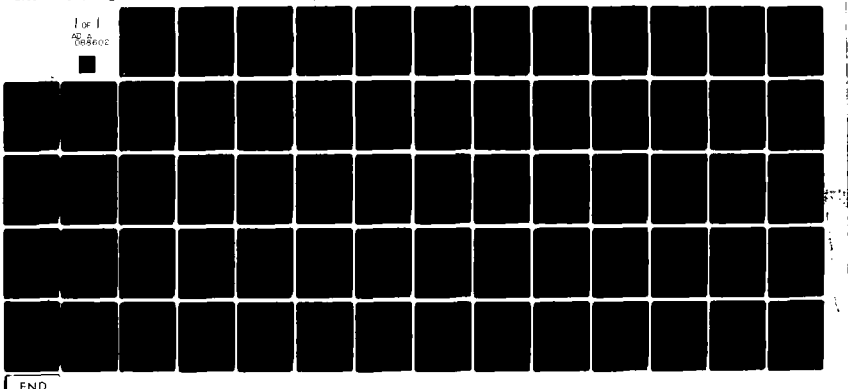

END
DATE FILMED
10-80
DTIC

SECURITY CLASSIFICATION OF THIS PAGE (When Data Entered)

REPORT DOCUMENTATION PAGE

READ INSTRUCTIONS BEFORE COMPLETING FORM

1. REPORT NUMBER	2. GOVT ACCESSION NO. A088602
3. RECIPIENT'S CATALOG NUMBER	(9)
4. TITLE (and Subtitle) Quasisteady Viscous Flows,	5. TYPE OF REPORT & PERIOD COVERED Final Report. Jan. 1, 1980-July 31, 1980
	6. PERFORMING ORG. REPORT NUMBER 1 Jan-31 Jul. 19
7. AUTHOR(s) (10) Paul Gordon	8. CONTRACT OR GRANT NUMBER(s) (15) N00014-78-C-0308 NR 061-254
9. PERFORMING ORGANIZATION NAME AND ADDRESS Purdue University Calumet Hammond, IN 46323 Campus	10. PROGRAM ELEMENT, PROJECT, TASK AREA & WORK UNIT NUMBERS NR 061-254
11. CONTROLLING OFFICE NAME AND ADDRESS U.S. Office of Naval Research Fluid Dynamics Branch 800 N. Quincy St., Arlington, VA 22217	12. REPORT DATE July 31, 1980
	13. NUMBER OF PAGES 59
14. MONITORING AGENCY NAME & ADDRESS(if different from Controlling Office) 9-1 Jul 89 (12)	15. SECURITY CLASS. (of this report) Unclassified
	15a. DECLASSIFICATION/DOWNGRADING SCHEDULE

16. DISTRIBUTION STATEMENT (of this Report)

Approved for public release; distribution unlimited.

17. DISTRIBUTION STATEMENT (of the abstract entered in Block 20, if different from Report)

18. SUPPLEMENTARY NOTES

SEP 3 1980

A

19. KEY WORDS (Continue on reverse side if necessary and identify by block number)

quasisteady models, viscous flows, boundary layers

20. ABSTRACT (Continue on reverse side if necessary and identify by block number)

In earlier work the author has applied quasisteady analysis to inviscid atmospheric flow. The goal of such analysis is to obtain simplified mathematical models which are consistent with both the original model and the physical scale of the problem. In the present paper this approach is applied to time-dependent viscous flows. The basic model consists of Cauchy's Equations in which relaxation equations are used to model the viscous

DD FORM 1 JAN 73 1473 EDITION OF 1 NOV 65 IS OBSOLETE

411907

SECURITY CLASSIFICATION OF THIS PAGE (When Data Entered)

20. parameters. Quasisteady models are obtained for the one and two dimensional cases, and specific application is made to both compressible and incompressible boundary layer situations. Several analytical and numerical solutions are obtained for the incompressible models.

Quasisteady Viscous Flows

I Introduction

In an earlier paper [1] the author showed the following: In an internal region of the flow where significant variations occur only over many mean-free paths, the viscous terms of the compressible Navier-Stokes Equations provide only a small perturbation on the forces described by the inviscid equations. This conclusion, although consistent with known results concerning strong shocks and thin boundary layers, presents difficulties in regard to incompressible flows. In [1] the following was stated:

> ... there exist many calculations, with the incompressible Navier-Stokes Equations, in which the viscous effects are pronounced and yet significant variations occur only over many mean-free paths. The analysis of the present paper indicates that the use of the time-dependent incompressible Navier-Stokes equations in these situations is totally unjustified.

However, no resolution of this problem was offered.

In later work [2,3] the author considered atmospheric inviscid flows. The atmospheric problem is not unlike the incompressible boundary layer situation: The hydrostatic assumption in atmospheric models is much like the assumption $\frac{\partial p}{\partial z} = 0$ of incompressible models. In [2,3] the approach was to use quasisteady analysis to obtain simplified mathematical models which are, 1) consistent with the scale of the physical problem, and 2) consistent with the original mathematical model. The results of these investigations leads one to conclude that quasisteady analysis is both valid and useful.

In order to use the approach of the atmospheric problem, it is necessary that the mathematical model consist of a system of first order hyperbolic partial differential equations. For viscous flows such a model exists in the form of Cauchy's Equations if an appropriate specification is made for the viscous parameters. The purpose of the present paper is to apply quasisteady analysis to Cauchy's Equations, in which relaxation equations are used to model the viscous terms.

Section II considers two relatively simple situations , both of which will be needed in the later analysis: 1) a single hyperbolic equation with a forcing term, and 2) the non-Fourier heat conduction equation. In Sections III and IV quasisteady models are obtained from Cauchy's Equations of motion for, respectively, the one-dimensional and two-dimensional cases. Section V considers the problem of specifying boundary conditions. In Section VI application is made to boundary layer situations for both the compressible and incompressible cases. Some conparison is made between these models and existing models. Finally, Section VII discusses several analytical and numerical solutions to the incompressible case.

Section II: Examples Using Quasisteady Analysis

Two examples are considered in this section. Both will be needed in the later analysis of the viscous equations.

A) A Single Hyperbolic Equation with a forcing Term

The following equation is to be considered:

$$\theta_t + c\theta_x = f(\theta, x, t). \tag{1.1}$$

Two distinct phenomena are involved in this equation:

(i) The hyperbolic effect - through c, the "sound speed", information is transmitted from the boundaries to interior points of the region.

(ii) The forcing effect - the forcing term, f, does not transmit, but rather "creates" information as a *point source*.

Each effect occurs at its own rate. Our specific interest was in the consideration of quasi-steady situations related to these rates. One typical special case of eq.(1.1) is the following:

$$\theta_t + c\theta_x = -\frac{\theta-\theta_0}{t_1} \tag{1.2}$$

where c, θ_0, and t_1 are positive constants and $0 < x < L$. The characteristic curves of the hyperbolic system have slope $\frac{dt}{dx} = \frac{1}{c}$. Thus, a unique solution is determined by initial data and a boundary condition at $x = 0$. Considering only the boundary condition,

$$\theta(t,0) = \theta_1(t) + \theta_0, \tag{1.3}$$

the solution for $t > \frac{x}{L}$ can be written as,

$$\theta(t,x) = e^{-(\frac{x}{ct_1})}\ \theta_1(t - \tfrac{x}{c}) + \theta_o. \tag{1.4}$$

Suppose first, that the hyperbolic term is dominant. That is, assume

$$\frac{L}{ct_1} << 1. \tag{2.1}$$

Also, suppose the boundary data varies slowly. That is, assume

$$|\theta_1(t) - \theta_1(t - \tfrac{L}{c})| \text{ is negligible for all } t. \tag{2.2}$$

(This assumption was also important in our earlier work, [2, assumption (2)]). Then, from eqs. (1.4), (2.1), and (2.2),

$$\theta(t,x) \sim \theta_1(t - \tfrac{x}{c}) + \theta_0 \sim \theta_1(t) + \theta_0. \tag{2.3}$$

Returning to eq. (1.2), the quasi-steady solution is,

$$\theta_x = -\frac{\theta-\theta_0}{t_1 c} \qquad \text{or} \quad \theta(t,x) \sim \theta_1(t) + \theta_0. \tag{2.4}$$

Thus, assumptions (2.1) and (2.2) lead to a meaningful quasi-steady solution.

Suppose next that the forcing term is dominant. That is, suppose

$$\frac{L}{ct_1} >> 1. \tag{2.5}$$

Then, from eq. (1.4), $\theta(t,x) \sim \theta_0$ except near $x = 0$; at $x = 0$, $\theta(t,0) = \theta_1(t) + \theta_0$. We see then that the dominance of the forcing term produces a boundary layer effect unless $\theta_1(t) = 0$. Furthermore, in this case a quasi-steady solution would not be valid near the boundary. If $\theta_1(t) \equiv 0$, the solution is simply $\theta_x = 0$, or $\theta \equiv \theta_0$. The latter situation will arise in the study

of the pressure equation in Section V.

B) The Non-Fourier Heat Conduction Equation

The heat conduction equation,

$$T_t = kT_{xx},\ 0 < x < L,\ t > 0, \tag{3.1}$$

involves the assumption,

$$q = -kT_x. \tag{3.2}$$

That eq.(3.2) is a quasi-steady equation is a fact that was heavily emphasized by early researchers (see, for example, Maxwell [4]). The following non-quasi-steady equation, or non-Fourier equation, has been investigated by various people; see, for example, refs. 5 and 6:

$$\begin{aligned} T_t &= -q_x \\ q_t &= -\frac{1}{t_1}(kT_x + q). \end{aligned} \tag{3.3}$$

In vector form we obtain:

$$\begin{aligned} V_t &= AV_x + BV, \\ V = \begin{pmatrix} T \\ q \end{pmatrix},\quad A &= \begin{pmatrix} 0 & -1 \\ -k/t_1 & 0 \end{pmatrix},\quad B = \begin{pmatrix} 0 & 0 \\ 0 & -1/t_1 \end{pmatrix}. \end{aligned} \tag{3.4}$$

Eqs. (3.4) and (1.2) have the same form. Letting

$$c^2 = \frac{k}{t_1}, \tag{4.1}$$

the matrix A has eigenvalues $\pm c$ with corresponding characteristics of slope $\pm \frac{1}{c}$. Also, the matrix B has the eigenvalues $0, \frac{1}{t_1}$. It follows, then, that both characteristic speeds for

the hyperbolic system have the same magnitude, namely $\frac{1}{c}$; however, the forcing term always has a zero eigenvalue, although the other may become large. As in eq. (1.2), it is first necessary to compare the magnitudes of c and t_1.

Eq. (3.4) is very interesting and was studied in some depth. Complete details will not be given here. A major difference between eqs. (3.4) and (1.2) is that in the latter c and t_1 can be considered independent quantities while in eq. (3.4) they are related through eq. (4.1). There are three time scales to consider:

$$\Delta t_1 = t_1: \quad \text{forcing term scale,} \tag{4.2}$$

$$\Delta t_2 = \Delta x/c: \quad \text{hyperbolic scale,} \tag{4.3}$$

$$\Delta t_3 = \Delta x^2/k: \quad \text{parabolic scale} \tag{4.4}$$

Δx is not here intended as a numerical quantity, but rather as some physically significant length. In order to take a quasi-steady limit with respect to the forcing term, we would need

$$\Delta t_1 = \varepsilon \Delta t_2, \ \varepsilon \text{ small.} \tag{5.1}$$

[Eq. (5.1) should be compared with eq. (2.5)]. From eqs. (4), we obtain $\Delta t_2^2 = \frac{\Delta x^2}{c^2} = \frac{\Delta x^2 t_1}{k} = \Delta t_1 \, \Delta t_3$. Then, from eq. (5.1),

$$\Delta t_2 = \varepsilon \Delta t_3 \ . \tag{5.2}$$

Suppose a physical situation is such that a priori one knows that Δt_3 is the appropriate time scale. If, then, ε is small, the quasi-steady solution requires that in eq. (3.4) $V_t \equiv 0$, or we obtain the steady-state solution to eq. (3.4).

Such a solution can be valid; the requirement is that boundary conditions for eq. (3.1) vary slowly with time, in the sense of eq. (2.2).

The general situation, however, would be that ε, of eq. (5.2) is small, but the steady-state solution is not valid. This means that it is not possible to independently take quasi-steady limits of the forcing term or the hyperbolic term. Apparently, if ε is small, the forcing term effect occurs more rapidly than the hyperbolic effect, but both disappear in the limit of $\varepsilon = 0$. This situation is still somewhat unclear. The different eigenvalues of the matrix B are a factor here. Analytic solutions were obtained for specific problems, such as $T(t,0) = T(t,L) = 0$. These solutions indicate that the limit $t_1 \to 0$ of the solution of eq. (3.3) does approach the solution of eq. (3.1), although convergence is somewhat "precarious".

The opposite case, $\varepsilon \sim 1$, is also surprising, but more informative. In this case, since $\Delta t_1 \sim \Delta t_2 \sim \Delta t_3$, the relaxation effect occurs on the same scale as the other effects and consequently cannot be deleted.

The above analysis is directly applicable to the Navier-Stokes Equations in the following ways:

i) The situation of $\varepsilon \sim 1$ will correspond to a "mesh Renolds Number" of approximately 1.

ii) The two-dimensional viscous equations have a "subsystem" with precisely the form of eq. (3.4).

Section III: The One-Dimensional Viscous Flow Equations

The one-dimensional equations of motion, Cauchy's equation, [7] are as follows:

$$\begin{aligned} &\rho_t + u\rho_x + \rho u_x = 0, \\ &\rho(u_t + uu_x) + p_x = \sigma_x, \\ &\rho c_v(T_t + uT_x) + pu_x = -q_x + \sigma u_x. \end{aligned} \tag{6}$$

Where p = pressure, ρ = density, u = x component of velocity, T = temperature, t = time coordinate, x = distance coordinate, c_v = specific heat, q = heat flux, σ = shear stress.
Upon introducing the quasi-steady assumptions,

$$q = -kT_x, \tag{7.1}$$

$$\sigma = \mu u_x, \tag{7.2}$$

$$p = \rho RT, \tag{7.3}$$

eq. (6) becomes the classical Navier-Stokes Equations. In the following, we introduce relaxation terms into eqs. (7.1) and (7.2):

$$\begin{aligned} \rho_t &= -u\rho_x - \rho u_x, \\ u_t &= -uu_x - \frac{p_t}{\rho} T_x - \frac{p_\rho}{\rho} \rho_x + \frac{1}{\rho} \sigma_x, \\ T_t &= -uT_x - \frac{1}{\rho c_v} q_x - \frac{p-\sigma}{\rho c_v} u_x, \\ q_t &= -uq_x - \frac{k}{t_1} T_x - \frac{q}{t_1}, \\ \sigma_t &= -u\sigma_x + \frac{\mu}{t_2} u_x - \frac{\sigma}{t_2}, \\ p &= p(\rho, T). \end{aligned} \tag{8}$$

where k = coefficient of thermal conductivity, μ = coefficient of shear viscosity, and t_1 and t_2 are relaxation times. In vector form,

$$V_t = -AV_x - F, \quad V = \begin{pmatrix} \rho \\ u \\ T \\ q \\ \sigma \end{pmatrix}, \quad F = \begin{pmatrix} 0 \\ 0 \\ 0 \\ q/t_1 \\ \sigma/t_2 \end{pmatrix} \tag{9}$$

$$A = \begin{pmatrix} u & \rho & 0 & 0 & 0 \\ p_\rho/\rho & u & p_T/\rho & 0 & -1/\rho \\ 0 & \frac{p-\sigma}{\rho c_v} & u & 1/\rho c_v & 0 \\ 0 & 0 & k/t_1 & u & 0 \\ 0 & -\mu/t_2 & 0 & 0 & u \end{pmatrix}$$

Various features of eq. (9) were studied. First, the eigenvalues of A were found to be the solution of the following equation in λ:

$$(u - \lambda)[(u - \lambda)^4 - a(u - \lambda)^2 + b] = 0 \tag{10.1}$$

where

$$a = c_q^2 + c_\sigma^2 + c_s^2 - \frac{\sigma}{p} c_T^2, \quad b = c_q^2(c_\sigma^2 + c_\rho^2),$$

$$c_s^2 = c_\rho^2 + c_T^2, \quad c_\rho^2 = p_\rho, \quad c_T^2 = \frac{pp_T}{\rho^2 c_v},$$

$$c_q^2 = \frac{k}{\rho c_v t_1}, \quad c_\sigma^2 = \frac{\mu}{\rho t_2} .$$

In order that eq. (9) be hyperbolic it is sufficient that the roots of eq. (10) be real and distinct. A necessary condition, since $b > 0$, is that,

$$a > 0. \tag{10.2}$$

A complete analysis of eq. (10.2) would require specific information regarding the relaxation times t_1 and t_2. Although such an analysis will not be attempted here, eq. (10.2) can be considered a restriction on the parameters t_1 and t_2.

Assuming eq. (10.2), eq. (9) will be hyperbolic if,

$$a^2 - 4b > 0 \tag{10.3}$$

Various special cases were examined. For example, since

$$a^2 - 4b = (a - 2c_q^2)^2 + 4c_q^2 c_T^2 (1 - \frac{\sigma}{p}), \tag{10.4}$$

eq. (10.3) is satisfied in the special cases where $\frac{\sigma}{p} < 1$ or $c_T = 0$. Also, intuitively there is reason to suppose that c_s, c_q, and c_σ are comparable quantitities. If one assumes $c_s = c_q = c_\sigma = c$ then $a^2 - 4b = (c^2 - \frac{\sigma}{p} c_\sigma^2) + 4c_q^2 c_T^2 (1 - \frac{\sigma}{p})$. If one further assumes that $p = \rho RT$ and that $\sigma = 0$, then $a^2 - 4b = c^4 [1 + \frac{4(\gamma-1)}{\gamma}]$. Letting $\gamma = 1.4$, the eigenvalues are found to be $\lambda = u,\ u \pm 1.494c,\ u \pm .8764c$.

It is not of course intended that the above be a definitive study of assumptions (10.2) and (10.3). Nevertheless, at this point it is reasonable to suppose that eq. (9) is hyperbolic for many, if not all, cases of interest. In particular, this is so for the incompressible limit $c_T = 0$.

Secondly, the normalized variables were considered [8]. This is a somewhat complex study, in that the diagonalizing

matrix for A needs to be found (as well as its inverse). The result is that the normalized variables for eq. (9) are comparable to those obtained in ref. 8 for the inviscid equations. This was considered important since the implication is that perturbation properties for eq. (9) are similar to those for the inviscid equations.

Thirdly, it is necessary to find a set of variables for which the eigenvalue corresponding to $\lambda = u$ is in some sense uncoupled from those involving the sound speed. Assuming that

$$\frac{t_2}{\mu} = \text{constant}, \tag{11}$$

a suitable set is,

$$W = \begin{pmatrix} \rho^* \\ u \\ T \\ q \\ \sigma^* \end{pmatrix}, \quad \rho^* = \rho e^{\frac{t_2}{\mu}\sigma}, \quad \sigma^* = p - \sigma . \tag{12.1}$$

Then

$$W_t = -A_1 W_x - B_1 W,$$

$$A_1 = \begin{pmatrix} u & 0 & 0 & 0 & 0 \\ 0 & u & 0 & 0 & 1/\rho \\ 0 & \frac{\sigma^*}{\rho c_v} & u & 1/\rho c_v & 0 \\ 0 & 0 & k/t_1 & u & 0 \\ 0 & \alpha & 0 & \frac{p_T}{\rho c_v} & u \end{pmatrix} \tag{12.2}$$

$$\alpha = \rho p_\rho + \frac{\sigma^*}{\rho c_v} p_T + \frac{\mu}{t_2}$$

$$B_1 = \text{Diag.}\{ \frac{\sigma}{\mu}, 0, 0, \frac{1}{t_1}, \frac{-\sigma}{t_2} \}$$

Remark: If assumption (11) does not hold, it may not be possible in all cases to achieve an uncoupled form through an analytic transformation. This does not affect the validity of the quasisteady equations, but the analysis needs to be considerably modified. It is of interest to note that the term $\rho^* \frac{\sigma}{\mu}$, which in the steady-state limit reduces to ρu_x, is now a forcing term, and not part of the hyperbolic effect.

Finally, the possibility of quasisteady solutions was considered. If a quasisteady situation exists relative to the various "sound" speeds and if the flow velocity is small relative to these speeds, then one must use the steady-state form of the last four equations. The system is then,

$$\rho^*_t = -u\rho^*_x - \rho^* u_x \ , \tag{13.1}$$

$$0 = -uu_x - \frac{1}{\rho}(p - \mu u_x)_x , \tag{13.2}$$

$$0 = -\left(\frac{p-\mu u_x}{\rho c_v}\right)u_x - uT_x + \frac{k}{\rho c_v} T_{xx} \ . \tag{13.3}$$

If we then let $t_2 \to 0$, eq. (13.1) becomes the continuity equation. Summarizing, the momentum and energy equations are in quasi-steady equilibrium with respect to the continuity equations. In addition, a condition such as eq. (2.2) is also implied for validity of eqs. (13).

Suppose next that the length of interest is small; that is, suppose

$$\Delta x \sim \lambda = \text{mean-free path} = \frac{\mu}{\rho c_s} \ , \tag{14.1}$$

where Δx is again intended as a physically significant length. Suppose also that the relaxation times are on the order of the time required to traverse a mean-free path at the sound speed,

$$t_1 \sim t_2 \sim \frac{\lambda}{c_s} \tag{14.2}$$

$$c_\sigma^2 = \frac{\mu c_s}{\rho \lambda} = c_s^2 , \tag{14.3}$$

$$c_q^2 = \frac{k c_s}{\rho c_v \lambda} = \left(\frac{k}{\mu c_v} \right) c_s^2, \tag{14.4}$$

where, as noted in [1], $\frac{\mu c_v}{k}$ is essentially a Prandtl number. If this Prandtl number is near unity, then $c_q \sim c_s = c_\sigma = c$, and the hyperbolic time scale for the problem, $\Delta t \sim \frac{\lambda}{c}$, is comparable to the forcing time scale t_1.

If u is comparable to c, then in this case, as in the discussion of the heat conduction equation, eq. (12) should be used as it is. Under assumptions (14.1) and (14.2), eq. (12) is on the same order of difficulty, in terms of obtaining a numerical solution, as the usual inviscid system. One expects the solution to steady-state flows to be similar to those obtained from the Navier-Stokes Equations. On the other hand, solutions to time-dependent flows (such as shock interaction problems) could be considerably altered.

If $|u| << c$, then eqs. (13) could be a feasible set of quasisteady equations.

Section IV: The Two-Dimenstional Viscous Flow Equations

The Cauchy equations now take the following form:

$$\begin{aligned}
&\rho_t + u\rho_x + w\rho_z + \rho u_x + \rho w_z = 0,\\
&\rho(u_t + uu_x + wu_z) + p_x = \tau_z + \sigma^*_x,\\
&\rho(w_t + uw_x + ww_z) + p_z = \tau_x + \sigma^{**}_z,\\
&\rho c_v(T_t + uT_x + wT_z) + p(u_x + w_z) = -q^*_x\\
&\qquad -q^{**}_z + \sigma^* u_x + \tau(w_x + u_z) + \sigma^{**} w_z,
\end{aligned} \tag{15.1}$$

where u, w are velocity components in the x,z directions, respectively, q* and q** are the components of the heat flux, and the 2x2 stress matrix has the form $\begin{pmatrix}\sigma^* & \tau\\ \tau & \sigma^{**}\end{pmatrix}$, see ref. 9, p. 46. Using

$$\begin{aligned}
&\tau = \mu(w_x + u_z),\\
&\sigma^* = \mu[2u_x - \tfrac{2}{3}(u_x + w_z)]\\
&\sigma^{**} = \mu[2w_z - \tfrac{2}{3}(u_x + w_z)]\\
&q^* = -kT_x \text{ and } q^{**} = -kT_z
\end{aligned} \tag{15.2}$$

Eq. (15.1) becomes the compressible Navier-Stokes Equations.

As in [2] and [3], the top of the region will be allowed to float so as to remain a streamline. This is accomplished by the transformation,

$$\tilde{t} = t, \tag{16.1}$$

$$\eta = x, \tag{16.2}$$

$$\zeta = \frac{z - f_1(t,x)}{f_2(t,x) - f_1(t,x)} \tag{16.3}$$

with

$$(f_2)_t = w + u\left(\frac{\zeta_x}{\zeta_z}\right), \tag{16.4}$$

where f_1 and f_2 represent, respectively, the position of the lower and upper boundaries.

If we then also add relaxation parameters to the viscous terms, eqs. (15) become:

$$\rho_{\tilde{t}} + u\rho_\eta + r\rho_\zeta + \rho(u_\eta + u_\zeta\zeta_x) + \rho\zeta_z w_\zeta = 0, \tag{17.1}$$

$$\rho(u_{\tilde{t}} + uu_\eta + ru_\zeta) + p_\eta + p_\zeta\zeta_x = \zeta_z\tau_\zeta + \sigma^*_\eta + \sigma^*\zeta_x, \tag{17.2}$$

$$\rho(w_{\tilde{t}} + uw_\eta + rw_\zeta) + p_\zeta\zeta_z = \zeta_z\sigma^{**}_\zeta + \tau_\eta + \tau_\zeta\zeta_x, \tag{17.3}$$

$$\begin{aligned}\rho c_v(T_{\tilde{t}} + uT_\eta + rT_\zeta) + p(u_\eta + u_\zeta\zeta_x + w_\zeta\zeta_z) = \\ -(q^*_\eta + q^*_\zeta\zeta_x) - q^{**}_\zeta\zeta_z + \sigma^*(u_\eta + u_\zeta\zeta_x) \\ + \tau(w_\eta + w_\zeta\zeta_x + u_\zeta\zeta_z) + \sigma^{**}w_\zeta\zeta_z,\end{aligned} \tag{17.4}$$

$$\tau_{\tilde{t}} + u\tau_\eta + r\tau_\zeta = \frac{\mu(w_\eta + w_\zeta\zeta_x + u_\zeta\zeta_z) - \tau}{t_1} \tag{17.5}$$

$$\sigma^*_{\tilde{t}} + u\sigma^*_\eta + r\sigma^*_\zeta = \frac{\mu[\frac{4}{3}u_\eta + \frac{4}{3}u_\zeta\zeta_x - \frac{2}{3}w_\zeta\zeta_z] - \sigma^*}{t_2} \tag{17.6}$$

$$\sigma^{**}_{\tilde{t}} + u\sigma^{**}_\eta + r\sigma^{**}_\zeta = \frac{\mu[\frac{4}{3}w_\zeta\zeta_z - \frac{2}{3}u_\eta - \frac{2}{3}u_\zeta\zeta_x] - \sigma^{**}}{t_3} \tag{17.7}$$

$$q^*_{\tilde{t}} + uq^*_\eta + rq^*_\zeta = \frac{-k(T_\eta + T_\zeta\zeta_x) - q^*}{t_4} \tag{17.8}$$

$$q^{**}_{\tilde{t}} + uq^{**}_\eta + rq^{**}_\zeta = \frac{-kT_\zeta\zeta_z - q^{**}}{t_5} \tag{17.9}$$

where

$$r = \zeta_t + u\zeta_x + w\zeta_z.$$

The variable propagating at the flow velocity is uncoupled from the system by defining,

$$\rho^* = \rho e^{\left(\frac{3t_2}{2\mu}\sigma^* + \frac{3t_3}{2\mu}\sigma^{**}\right)} \tag{18.1}$$

$$\bar{\sigma}^* = p - \sigma^*, \tag{18.2}$$

$$\bar{\sigma}^{**} = p - \sigma^{**} \tag{18.3}$$

With assumption (11), namely that $\frac{t_2}{\mu}$ and $\frac{t_3}{\mu}$ are both constant, eqs. (17) become,

$$\rho^*_{\tilde{t}} + u\rho^*_\eta + r\rho^*_\zeta = -\frac{3\rho^*}{2\mu}(\sigma^* + \sigma^{**}), \tag{19.1}$$

$$\rho(u_{\tilde{t}} + uu_\eta + ru_\zeta) = \zeta_z\tau_\zeta - \bar{\sigma}^*_\eta - \zeta_x\bar{\sigma}^*_\zeta, \tag{19.2}$$

$$\rho(w_{\tilde{t}} + uw_\eta + rw_\zeta) = \tau_\eta + \zeta_x\tau_\zeta - \zeta_z\bar{\sigma}^{**}_\zeta \tag{19.3}$$

$$\begin{aligned}\rho c_v(T_{\tilde{t}} + uT_\eta + rT_\zeta) = &-\bar{\sigma}^*u_\eta - \bar{\sigma}^*\zeta_x u_\zeta - \bar{\sigma}^{**}\zeta_z w_\zeta \\ &+ \tau(w_\eta + \zeta_x w_\zeta + \zeta_z u_\zeta) - (q^*_\eta + \zeta_x q^*_\zeta + \zeta_z q^{**}_\zeta),\end{aligned} \tag{19.4}$$

$$\begin{aligned}\bar{\sigma}^*_{\tilde{t}} + u\bar{\sigma}^*_\eta + r\bar{\sigma}^*_\zeta = &-\rho c_1^2 u_\eta - \rho(\zeta_x c_1^2 - \frac{\tau\zeta_z}{p}c_T^2)u_\zeta + \frac{\tau\rho}{p}c_T^2 w_\eta \\ &- \rho\zeta_z(c_2^2 - \frac{\zeta_x\tau c_T^2}{\zeta_z p})w_\zeta - \frac{\rho c_T^2}{p}(q^*_\eta + \zeta_x q^*_\zeta + \zeta_z q^{**}_\zeta) + \frac{\sigma^*}{t_2}\end{aligned} \tag{19.5}$$

$$\begin{aligned}\bar{\sigma}^{**}_{\tilde{t}} + u\bar{\sigma}^{**}_\eta + r\bar{\sigma}^{**}_\zeta = &-\rho c_3^2 u_\eta - \rho(\zeta_x c_3^2 - \frac{\tau\zeta_z}{p}c_T^2)u_\zeta + \frac{\tau\rho}{p}c_T^2 w_\eta \\ &- \rho\zeta_z(c_4^2 - \frac{\zeta_x\tau c_T^2}{\zeta_z p})w_\zeta - \frac{\rho c_T^2}{p}(q^*_\eta + \zeta_x q^*_\zeta + \zeta_z q^{**}_\zeta) + \frac{\sigma^{**}}{t_3},\end{aligned} \tag{19.6}$$

where

$$c_1^2 = p_\rho + \frac{\bar{\sigma}^*}{p} c_T^2 + \frac{4\mu}{3\rho t_2}, \tag{19.7}$$

$$c_2^2 = p_\rho + \frac{\bar{\sigma}^{**}}{p} c_T^2 + \frac{4\mu}{3\rho t_2}, \tag{19.8}$$

$$c_3^2 = p_\rho + \frac{\bar{\sigma}^*}{p} c_T^2 - \frac{2\mu}{3\rho t_3}, \tag{19.9}$$

$$c_4^2 = p_\rho + \frac{\bar{\sigma}^{**}}{p} c_T^2 + \frac{4\mu}{3\rho t_3}, \tag{19.10}$$

$$c_T^2 = \frac{pp_T}{\rho^2 c_v} \tag{19.11}$$

Eqs. (17.5), (17.8), and (17.9) are unchanged.

Suppose that solutions are desired in the region,

$$0 \leq \eta \leq L,\ 0 \leq \zeta \leq 1,\ \tilde{t} > 0 \tag{20.1}$$

Some simplification in eq. (19) is obtained by assuming that the vertical height and vertical variation is small:

$$|f_2 - f_1| \leq \text{several hundred mean-free paths}, \tag{20.2}$$

$$\frac{1}{L} |(f_2 - f_1)_\eta| << 1. \tag{20.3}$$

From (20.2) we assume that vertical velocities and pressure gradients are small. In particular, we assume:

$$|\frac{\zeta_x}{\zeta_z} w_\zeta| << |u_\zeta|, \tag{20.4}$$

$$|\frac{\zeta_x}{\zeta_z} p_\zeta| << |p_\eta| . \tag{20.5}$$

We therefore delete $w_\zeta \zeta_x$ from eq. (17.5) and $\bar{\sigma}^*_\zeta \zeta_x$ from eq. (19.2).

The equations then take the following form:

$$V_t = -AV_\eta - BV_\zeta - CV, \tag{21}$$

where

$$V = (\rho^*, w, T, q^*, q^{**}, \bar{\sigma}^{**}, \bar{\sigma}^*, u, \tau),$$

$$A = \begin{pmatrix}
u & 0 & 0 & 0 & 0 & 0 & 0 & 0 & 0 \\
0 & u & 0 & 0 & 0 & 0 & 0 & 0 & -\frac{1}{\rho} \\
0 & -\frac{\tau}{\rho c_v} & u & \frac{1}{\rho c_v} & 0 & 0 & 0 & \frac{\bar{\sigma}^*}{\rho c_v} & 0 \\
0 & 0 & \frac{k}{t_4} & u & 0 & 0 & 0 & 0 & 0 \\
0 & 0 & 0 & 0 & u & 0 & 0 & 0 & 0 \\
0 & -\frac{\tau\rho c_T^2}{p} & 0 & \frac{\rho c_T^2}{p} & 0 & u & 0 & \rho c_3^3 & 0 \\
0 & -\frac{\tau\rho c_T^2}{p} & 0 & \frac{\rho c_T^2}{p} & 0 & 0 & u & \rho c_1^2 & 0 \\
0 & 0 & 0 & 0 & 0 & 0 & \frac{1}{\rho} & u & 0 \\
0 & -\frac{\mu}{t_1} & 0 & 0 & 0 & 0 & 0 & 0 & u
\end{pmatrix}$$

$$B = \begin{pmatrix} r & 0 & 0 & 0 & 0 & 0 & 0 & 0 & 0 \\ 0 & r & 0 & 0 & 0 & \frac{\zeta_z}{\rho} & 0 & 0 & -\frac{\zeta_x}{\rho} \\ 0 & b_2 & r & \frac{\zeta_x}{\rho c_v} & \frac{\zeta_z}{\rho c_v} & 0 & 0 & b_1 & 0 \\ 0 & 0 & \frac{k}{t_4}\zeta_x & r & 0 & 0 & 0 & 0 & 0 \\ 0 & 0 & \frac{k}{t_5}\zeta_z & 0 & r & 0 & 0 & 0 & 0 \\ 0 & b_4 & 0 & \frac{\rho c_T^2 \zeta_x}{p} & \frac{\rho c_T^2 \zeta_z}{p} & r & 0 & b_3 & 0 \\ 0 & b_6 & 0 & \frac{\rho c_T^2 \zeta_x}{p} & \frac{\rho c_T^2 \zeta_z}{p} & 0 & r & b_5 & 0 \\ 0 & 0 & 0 & 0 & 0 & 0 & 0 & r & -\frac{\zeta_z}{\rho} \\ 0 & 0 & 0 & 0 & 0 & 0 & 0 & -\frac{\mu}{t_1}\zeta_z & r \end{pmatrix}$$

$$C = \left(\frac{3(\sigma^* + \sigma^{**})}{2\mu}, 0, 0, \frac{-1}{t_4}, \frac{-1}{t_5}, \frac{-1}{t_3}, \frac{-1}{t_2}, 0, \frac{1}{t_1}\right)$$

$$b_1 = \frac{\bar{\sigma}^* \zeta_x - \tau \zeta_z}{\rho c_v}, \quad b_2 = \frac{\bar{\sigma}^{**} \zeta_z - \tau \zeta_x}{\rho c_v},$$

$$b_3 = \rho\left(\zeta_x c_3^2 - \frac{\tau \zeta_z c_T^2}{p}\right), \quad b_4 = \rho \zeta_z \left(c_4^2 - \frac{\zeta_x \tau c_T^2}{\zeta_z p}\right),$$

$$b_5 = \rho\left(\zeta_x c_1^2 - \frac{\tau \zeta_z c_T^2}{p}\right), \quad b_6 = \rho \zeta_z \left(c_2^2 - \frac{\zeta_x \tau c_T^2}{\zeta_z p}\right).$$

The solutions of $|B-\lambda I| = 0$ are $\lambda = r, r, r + \sqrt{\frac{\mu}{\rho t_1}}$, $r - \sqrt{\frac{\mu}{\rho t_1}}$, and the solutions of $|B_1-\lambda I| = 0$, where B_1 is the indicated 5x5 submatrix. The latter 5 are solutions of the polynomial,

$$(r - \lambda)[(r - \lambda)^2 - a(r - \lambda) + b] \tag{22}$$

where

$$a = \frac{\zeta_z}{\rho} b_4 + \frac{k}{\rho c_v t_5} \zeta_z^2 + \frac{k}{\rho c_v t_4} \zeta_x^2 ,$$

$$b = \left(\frac{k}{\rho c_v t_4} \zeta_z^2 + \frac{k}{\rho c_v t_5} \zeta_x^2 \right)\left(b_4 \frac{\zeta_z}{\rho} - \frac{b_2 \rho c_v \zeta_z c_T^2}{p} \right)$$

The discussion of the one-dimensional system given in Section III is applicable to eq. (22). In particular, we assume the following:

i) The solutions of the 4th degree polynomial in eq.(22) are

$$\lambda = r \pm \tilde{c}_1, \; r \pm \tilde{c}_2. \tag{23.1}$$

ii) $$|r| << c_h \quad \text{where } c_h = \min(\tilde{c}_1, \tilde{c}_2, \sqrt{\frac{\mu}{\rho t_1}}). \tag{23.2}$$

iii) As a consequence of assumption (20.2), the relaxation times are comparable to the hyperbolic time scale,

$$(f_2 \sim f_1)/c_h. \tag{23.3}$$

In the discussion of boundary conditions we will need the correspondence between eigenvalues and the variables. These are as follows:

i) $\lambda = r, \; r, \; r$ correspond to ρ^*, σ^*, and q^*, (24.1)

ii) $\lambda = r \pm \sqrt{\frac{\mu}{\rho t_1}}$ correspond to u and τ, (24.2)

iii) $\lambda = r \pm \tilde{c}_1, \; r \pm \tilde{c}_2$ correspond to w, T, q^{**}, and $\bar{\sigma}^{**}$. (24.3)

Remark: Eqs. (24) are not quite accurate in that the variables involved in the above matrix B_1 need to be modified so as to uncouple the variable corresponding to $\lambda = r$. However, because

of assumption (20.3), ζ_x is small and the appropriate variables will be small perturbations of the present ones. The result will not affect the final quasisteady equations and so the derivation is not carried out here.

The eigenvalues of the matrix A of eq. (21) are given by,

$$|A - \lambda I| = (u-\lambda)^3[(u-\lambda)^2 - \frac{\mu}{\rho t_1}][(u-\lambda)^4 - a(u-\lambda)^2 + b], \qquad (25)$$

where

$$a = c_1^2 + \frac{k}{\rho c_v t_4},$$

$$b = \frac{k}{\rho c_v t_4}(c_1^2 - \frac{\bar{\sigma}^* c_T^2}{p}).$$

The solutions of the 4th degree polynomial in eq. (25) are easily seen to be real. Consequently, the eigenvalues of A are $\{\lambda = u,u,u,\ u \pm \sqrt{\frac{\mu}{\rho t_1}},\ u \pm \tilde{c}_3,\ u \pm \tilde{c}_4\}$ where $\tilde{c}_3$ and $\tilde{c}_4$ correspond to the 4th degree polynomial. It is assumed that,

$$|u| < c_\ell = \min(\tilde{c}_3, \tilde{c}_4, \sqrt{\frac{\mu}{\rho t_1}}). \qquad (26)$$

The correspondence between eigenvalues and variables is as follows:

i) $\lambda = u, u, u$ correspond to $\rho^*, q^{**}, \bar{\sigma}^{**}$, (27.1)

ii) $\lambda = u \pm \sqrt{\frac{\mu}{\rho t_1}}$ correspond to w and τ, (27.2)

iii) $\lambda = u \pm \tilde{c}_3,\ u \pm \tilde{c}_4$ correspond to $T, q^*, \bar{\sigma}^*, u$. (27.3)

As in the atmospheric problem, the goal here is to consider quasisteady situations induced by "distortion" in the spatial scale; that is, we consider boundary layer situations. The physical scale assumptions for the present problem can be stated as follows [2, assumption 2]

i) The physical region, given by eq. (20.1), is such that $(f_2 - f_1)/c_h << L/c_\ell$. (28.1)

ii) Boundary conditions and initial conditions are such that the flow variables will experience significant variations only over time scales which are large compared to $(f_2 - f_1)/c_h$. (28.2)

Remark: Assumptions (28) would be typically satisfied in thin boundary layers. In many such problems the vertical mesh has caused severe numerical problems [10,11].

Because of assumption (28.1), we need not consider the possibility of simultaneously having quasisteady limits with respect to both η and ζ. By assumption (28.2), however, quasisteady limits with respect to ζ are feasible. We conclude, therefore, as follows: By eqs. (24.2) and (24.3) and assumption (23.2), the variables $\{u,\tau,w,T,q^{**},\bar{\sigma}^{**}\}$ are in quasisteady equilibrium with respect to ρ^*; by assumption (23.3), the variables $q^*,\bar{\sigma}^*$ are in quasisteady equilibrium with respect to ρ^*. The viscous parameters are then,

$$\tau = \mu(w_\eta + \zeta_z u_\zeta), \tag{29.1}$$

$$\sigma^* = \frac{4}{3}\mu(u_\eta + \zeta_x u_\zeta) - \frac{2}{3}\mu\zeta_z w_\zeta, \tag{29.2}$$

$$\sigma^{**} = \mu(\frac{4}{3} w_\zeta \zeta_z - \frac{2}{3} u_\eta - \frac{2}{3} \zeta_x u_\zeta), \tag{29.3}$$

$$q^* = -k(T_\eta + \zeta_x T_\zeta), \tag{29.4}$$

$$q^{**} = -kT_\zeta, \tag{29.5}$$

with the final partial differential equations as follows:

$$\rho_{\tilde{t}} + u\rho_\eta + r\rho_\zeta = -\rho(u_\eta + \zeta_x u_\zeta + \zeta_z w_\zeta), \tag{30.1}$$

$$0 = -\rho(uu_\eta + ru_\zeta) + \zeta_z\mu(w_\eta + \zeta_z u_\zeta)_\zeta - p_\eta + \sigma^*_\eta, \tag{30.2}$$

$$\begin{aligned} 0 = {} & -\rho(uw_\eta + rw_\zeta) + \tau_\eta + \zeta_x\mu(w_\eta + \zeta_z u_\zeta)_\zeta - \zeta_z p_\zeta \\ & + \zeta_z\mu\left(\tfrac{4}{3} w_\zeta\zeta_z - \tfrac{2}{3} u_\eta - \tfrac{2}{3} u_\zeta\zeta_x\right)_\zeta, \end{aligned} \tag{30.2}$$

$$\begin{aligned} 0 = {} & -\rho c_v(uT_\eta + rT_\zeta) + \left[\tfrac{4}{3}\mu(u_\eta + \zeta_x u_\zeta) - \tfrac{2}{3}\mu\zeta_z w_\zeta\right](u_\eta + \zeta_x u_\zeta) \\ & - p(\zeta_x u_\zeta + u_\eta) - p\zeta_z w_\zeta + \mu\left(\tfrac{4}{3} w_\zeta\zeta_z - \tfrac{2}{3} u_\eta - \tfrac{2}{3} u_\zeta\zeta_x\right)w_\zeta\zeta_z \\ & + \mu(w_\eta + \zeta_z u_\zeta)(w_\eta + \zeta_x w_\zeta + \zeta_z u_\zeta) + k(T_\eta + \zeta_x T_\zeta)_\eta \\ & + k\zeta_x(T_\eta + T_\zeta\zeta_x)_\zeta + \zeta_z^2 kT_{\zeta\zeta}, \end{aligned} \tag{30.4}$$

where in eq. (30.1) it has been assumed that $\rho^* \to \rho$.

Summarizing, the quasisteady equations (30) are proposed as an approximation to eqs. (17) if the several assumptions {20.2, 20.3, 20.4, 20.5, 23.1, 23.2, 23.3, 28.1, 28.2} are satisfied.

Section V: Boundary Equations for the Quasisteady Model

The approach used to obtain boundary equations for the quasisteady model will be the same as that described in [3]: First, at each boundary an appropriate set of characteristic equations and boundary conditions is specified for the time-dependent model; secondly, we attempt to simultaneously take the quasisteady limit of the internal partial differential equations and the boundary equations.

As a specific problem, we will consider viscous flow over a flat plate: $\eta = 0$ will represent a position somewhere downstream of the leading edge and $\zeta = 0$ represents the wall.

The nine equations needed at each boundary for the time-dependent model, eq. (21), will consist of boundary conditions (whose number is determined by the number of incoming characteristics) plus characteristic (linearized) equations.

We assume that,

$$\eta = 0 \text{ is an inflow boundary and } \eta = 1 \text{ is an outflow boundary (Except at } \zeta = 0,\ u = 0 \text{ at } \eta = 0 \text{ and } \eta = 1). \tag{31}$$

From eqs. (25), (26) and 30, at $\eta = 0$ six eigenvalues are positive, indicating six incoming characteristics, and three are negative. The nine equations can be chosen as

$$\rho = h_1(\tilde{t}, \zeta), \tag{32.1}$$

$$\left.\begin{aligned} q^{**} &= h_2(\tilde{t}, \zeta), \\ \bar{\sigma}^{**} &= h_3(\tilde{t}, \zeta), \\ w &= h_4(\tilde{t}, \zeta), \\ T &= h_5(\tilde{t}, \zeta), \\ u &= h_6(\tilde{t}, \zeta), \end{aligned}\right\} \tag{32.2}$$

where h_i are specified functions, plus the three characteristic equations which will have the form (see [3] for more detail):

$$\left.\begin{aligned} &a_{11}w_{\tilde{t}} + a_{12}\tau_{\tilde{t}} = a_{13} \\ &a_{21}T_{\tilde{t}} + a_{22}q^*_{\tilde{t}} + a_{23}\bar{\sigma}^*_{\tilde{t}} + a_{24}u_{\tilde{t}} = a_{25} \\ &a_{31}T_{\tilde{t}} + a_{32}q^*_{\tilde{t}} + a_{33}\bar{\sigma}^*_{\tilde{t}} + a_{34}u_{\tilde{t}} = a_{35} \end{aligned}\right\} \quad (32.3)$$

At $\eta = 1$ there are three incoming characteristics. The equations can be chosen as follows:

$$w = 0, \quad (33.1)$$

$$q^* = 0, \quad (33.2)$$

$$p_t = \frac{\gamma p}{c_s} u_t, \quad (33.3)$$

(see [3] for a further discussion of (33.3) as an outflow lateral boundary condition. The six characteristic equations will consist of the partial differential equations for $\rho^*_{\tilde{t}}$, $q^{**}_{\tilde{t}}$, $\bar{\sigma}^{**}_{\tilde{t}}$ and three equations of the form (32.3).

At $\zeta = 0$, $r \equiv 0$ or, referring to eqs. (22) and (23), the following equations can be chosen: ρ^*, $\bar{\sigma}^*$, and q^* can be calculated from their differential equations; the boundary conditions can be taken as,

$$\begin{aligned} u &= f_{1_t}\left(\frac{\zeta_x}{\zeta_z}\right), \\ w &= f_{1_t}/\left[1 + \left(\frac{\zeta_x}{\zeta_z}\right)^2\right], \\ T &= h_7(t,\eta), \end{aligned} \quad (34.1)$$

and the characteristic equations have the form,

$$\begin{aligned} a_{41}u_{\tilde{t}} + a_{42}\tau_{\tilde{t}} &= a_{43}, \\ a_{51}T_{\tilde{t}} + a_{52}w_{\tilde{t}} + a_{53}q^{**}_{\tilde{t}} + a_{54}\bar{\sigma}^{**}_{\tilde{t}} &= a_{55}, \\ a_{61}T_{\tilde{t}} + a_{62}w_{\tilde{t}} + a_{63}q^{**}_{\tilde{t}} + a_{64}\bar{\sigma}^{**}_{\tilde{t}} &= a_{65}. \end{aligned} \tag{34.2}$$

At $\zeta = 1$, we again have $r \equiv 0$. Thus, the equations for ρ^*, $\bar{\sigma}^*$, and q^* can be used. The characteristic equations will have the form (34.2) and the boundary conditions are chosen as,

$$\left.\begin{aligned} \tau &= 0, \\ q^{**} &= 0 \Rightarrow T_\zeta = 0. \end{aligned}\right\} \tag{34.3}$$

$$p_t = \frac{\gamma p}{c_s} u_t \tag{34.4}$$

(See [3] for a discussion of the last equation in the context of an upper boundary condition.)

Eqs. (24) were obtained by assuming that the variables $\{u, w, T, \tau, q^*, q^{**}, \bar{\sigma}^*, \bar{\sigma}^{**}\}$ were in quasisteady equilibrium with respect to ρ^*. Quasisteady boundary conditions are obtained by applying the following principles [2, eqs. (15 and (16)]:

> If a boundary equation involves any one of $\{u_{\tilde{t}}, w_{\tilde{t}}, T_{\tilde{t}}, \tau_{\tilde{t}}, q^*_{\tilde{t}}, q^{**}_{\tilde{t}}, \bar{\sigma}^*_{\tilde{t}}, \bar{\sigma}^{**}_{\tilde{t}}\}$ and if the equation is driven by flow conditions internal to the region of computation, then the equation will be put in quasisteady equilibrium. (35.1)

The basic quasisteady assumptions, (28.1) and (28.2) require that eqs. (29.1)-(29.4) and eqs. (30.2)-(30.4) be applied at all points of the lateral boundaries, except possibly at the corner points. (35.2)

The following is thereby obtained:

a) At $\eta = 0$, eqs. (32.2) are deleted because of (35.2) and eqs. (32.3) are deleted by (35.1). Thus, ρ is obtained from eq. (32.1) and the remaining variables are determined by quasisteady equations.

b) At $\eta = 1$, eqs. (33) and all characteristic equations, except the equation for ρ^*, are deleted because of (35.2). Thus, ρ is obtained from eq. (30.1) and the remaining variables are determined by quasi-steady equations.

c) At the upper and lower boundaries, $\zeta = 0$ and 1, the equations for $\bar{\sigma}^*$ and q^*, as well as eqs. (34.2) are deleted because of (35.1). Thus, ρ is obtained from eq. (30.1) at both $\zeta = 0$ and 1. Also eqs. (34.1) are retained at $\zeta = 0$ and eqs. (34.3) are retained at $\zeta = 1$. (the last equation in (34.3) is retained because it is intended as a simulation of external flow conditions [3]).

Summarizing, the proposed quasisteady model is as follows:

i) ρ is obtained at $\eta = 0$ from eq. (32.1) and at all other points from eq. (30.1).

ii) u is obtained from eq. (30.2) and the boundary conditions (34.1) at $\zeta = 0$ and $\tau = 0$ at $\zeta = 1$.

iii) w is obtained from eq. (30.3), the boundary conditions (34.1) at $\zeta = 0$, and a condition, to be discussed below, at $\zeta = 1$.

iv) T is obtained form eq. (30.4) and the boundary conditions $T = h(t,\eta)$, where h is specified, at $\zeta = 0$ and $T_\zeta = 0$ at $\zeta = 1$.

v) Eq. (16.4) is a first order hyperbolic partial differential equation in the variable f_2 (f_1 is specified) and, because of eq. (30), requires a boundary condition at $\eta = 0$. We will impose,

$$(f_2)_{\tilde{t}} \equiv 0 \quad \text{at } \eta = 0. \tag{36}$$

The third condition of eqs. (34.3), $p_t = \frac{\gamma p}{c_s} u_t$, has not been used. It is the missing condition for w. Its use requires an additional iteration between eqs. (16.4), (34.4), and the calculation of u given above.

Remark: Clearly, eqs. (30.2), (30.3), and (30.4) are coupled and would in fact need to be solved simultaneously. The above description of the model is intended to display the primary dependence between the variables and the differential equations.

Finally, we need to consider the corner points. As discussed briefly in [3], inconsistencies can arise here in regard to boundary conditions:

i) $\zeta = 0$, $\eta = 0$: ρ is specified by eq. (32.1), T is specified or $h_5(\tilde{t},0) = h_7(\tilde{t},0)$ - see eqs. (32.2) and (34.1), u and w are specified by eqs. (34.1).

ii) $\zeta = 1$, $\eta = 0$: ρ is specified by eq. (32.1) and the remaining conditions are $T_\zeta = 0$, $\tau = 0$, and $p_t = \frac{\gamma p u_t}{c_s{}^2}$.

iii) $\zeta = 0$, $\zeta = 1$: ρ is calculated from eq. (30.1), and the other variables are as at $\zeta = 0$, $\eta = 0$.

iv) $\zeta = 1$, $\eta = 1$: ρ is calculated from eq. (30.1), and the other variables are as at $\zeta = 1$, $\eta = 0$.

Section VI: Boundary Layer Approximations

Assumption (28.1) has the effect of requiring that the width of the region be small relative to the length. The following assumption insures that the length itself is large:

> L is large relative to the mean-free path, so that significant variations in the x-direction occur only over many mean-free paths. (37)

From the results in [1] we conclude that the viscous terms, in the η-direction, of the Navier-Stokes Equations can be deleted. Assuming this conclusion also holds for the Cauchy Equations, eqs. (30) reduce to the following:

$$\rho_{\tilde{t}} + u\rho_\eta + r\rho_\zeta = -\rho(u_\eta + \zeta_x u_\zeta + \zeta_z w_\zeta), \tag{38.1}$$

$$0 = -\rho(uu_\eta + ru_\zeta) + \zeta_z^2 \mu u_{\zeta\zeta} - p_\eta, \tag{38.2}$$

$$\begin{aligned} 0 = {} & -\rho(uw_\eta + rw_\zeta) + \zeta_x\zeta_z\mu u_{\zeta\zeta} - \zeta_z p_\zeta \\ & + \zeta_z\mu\left(\tfrac{4}{3}\,\zeta_z w_\zeta - \tfrac{2}{3}\,\zeta_x u_\zeta\right)_\zeta, \end{aligned} \tag{38.3}$$

$$\begin{aligned} 0 = {} & -\rho c_v(uT_\eta + rT_\zeta) - p(u_\eta + \zeta_x u_\zeta + \zeta_z w_\zeta) \\ & + \mu\zeta_z^2[u_\zeta^2 + \tfrac{4}{3}\,w_\zeta^2] + k\zeta_z^2\, T_{\zeta\zeta}, \end{aligned} \tag{38.4}$$

where, on the basis of assumptions (20.3) and (20.4), several viscous terms involving ζ_x have been deleted from eq. (38.4).

Remark: Assumption (37) could have been applied before making the transformation to $\{\tilde{t}, \eta, \zeta\}$. In this case the viscous terms involving ζ_x would not appear in eq. (38.3). This is consistent with the well-known result in boundary layer theory that the final approximation is dependent to a certain extent on the coordinate system.

Eqs. (38) are similar to Stokes' Equations for compressible flow [12, eqs. (20)], which are obtained as the limit of the Reynolds Number approaching zero. Letting,

$$M = \text{Mach Number} = \frac{u}{c_s}, \tag{39.1}$$

$$R_e = \text{Reynolds Number} = \frac{uL\rho}{\mu}, \tag{39.2}$$

$$\lambda = \text{mean-free path} = \frac{\mu}{\rho c}, \tag{39.3}$$

we obtain,

$$R_e = M(\frac{L}{\lambda}). \tag{39.4}$$

L/λ is large, by assumption (37), but there is as yet no restriction on M (assumption (26) was introduced only for the purpose of specifying boundary conditions). Thus, eqs. (38) are valid for large Reynolds Number, as long as the scale assumptions are satisfied.

Eqs. (38) should also be compared with the boundary equations commonly used for time dependent compressible flows, as, for example, given by Lagerstrom [12, eqs. (20-12)]. Very fundamental differences are seen:

i) Lagerstrom's equations retain the time derivative in the horizontal momentum equation and the energy equation, whereas both have been deleted in eq. (38).

ii) Lagerstrom's equations have replaced the vertical momentum equation with the condition $p_\zeta = 0$. In eqs. (38) a further assumption, to be discussed below, is required before such a simplification can be attempted.

An incompressible version of eqs. (38) is obtained by

assuming $P_T = 0$. Eq. (38.4) is then uncoupled from the remaining equations. With the notation,

$$p = p(\rho) \quad \text{and} \quad p_\rho = c^2, \tag{40.1}$$

eqs. (38) become,

$$p_{\tilde{t}} + up_\eta + rp_\zeta = -\rho c^2(u_\eta + \zeta_x u_\zeta + \zeta_z w_\zeta), \tag{40.2}$$

$$\rho(uu_\eta + ru_\zeta) - \zeta_z^2 \mu u_{\zeta\zeta} + p_\eta = 0, \tag{40.3}$$

$$\rho(uw_\eta + rw_\zeta) - \zeta_x\zeta_z uu_{\zeta\zeta} - \zeta_z\mu(\tfrac{4}{3}\zeta_z w_\zeta - \tfrac{2}{3}\zeta_x u_\zeta)_\zeta + \zeta_z p_\zeta = 0. \tag{40.4}$$

Eqs. (40) can be compared with, for example, Prandtl's boundary layer equations [9, eqs. (7.7) & (7.8)]. The essential differences would be as follows:

i) In Prandtl's equations, eqs. (40.2) and (40.4) will be replaced respectively by $u_\eta + \zeta_x u_\zeta + \zeta_z w_\zeta = 0$ and $p_\zeta = 0$.

ii) In Prandtl's equations, the time derivative term would be added to eq. (40.3).

Boundary equations for eqs. (40), corresponding to those given in Section V, would be as follows:

$$\zeta = 0: \quad u = f_{1_t}(\frac{\zeta_x}{\zeta_z}), \; w = f_{1_t}/[1 + (\frac{\zeta_x}{\zeta_z})^2], \text{ eq.(40.2)}; \tag{41.1}$$

$$\zeta = 1: \quad u_\zeta = 0, \; p_t = \frac{\gamma p}{c_s} u_t, \text{ eq. (40.2)}; \tag{41.2}$$

$$\eta = 0: \quad \rho \text{ specified, eqs. (40.3) and (40.4)}, \tag{41.3}$$

$$\eta = 1: \quad \text{eqs. (40.1), (40.2), (40.3)}. \tag{41.4}$$

A further simplification of eqs. (40) can be achieved by analyzing the time scales associated with these equations. Since, in the time dependent form, the right side of eq.(40.1)

is a forcing term, then with our assumptions the hyperbolic time scale for eq.(40.1) is,

$$\Delta t_1 = \frac{L}{u} \tag{42.1}$$

Integrating eq.(40.4) in the form,

$$\zeta_z w_\zeta = -\frac{\zeta_x}{4} u_\zeta + \frac{3}{4}(\zeta_x)_\zeta u + \frac{p-p^*}{\frac{4}{3}\mu} + b_1, \tag{42.2}$$

where

$$b_1 = \frac{3}{4\mu\zeta_z} \int_0^\zeta \rho(uw_\eta + rw_\zeta)d\tilde{\zeta},$$

$$p^* = p(\tilde{t}, \eta, 1),$$

and substituting into eq.(40.4), we obtain,

$$p_{\tilde{t}} + up_\eta + rp_\zeta = -\frac{p-p^*}{\Delta t_2} + b_2, \tag{42.3}$$

where

$$b_2 = -\rho c^2(u_\eta + \zeta_x u_\zeta + b_1),$$

$$\Delta t_2 = \frac{4\mu}{3\rho c^2} .$$

Next, defining w_ε and w^* by,

$$w = w^* + w_\varepsilon \tag{43.1}$$

and

$$\zeta_z w^*_\zeta = -(u_\eta + \zeta_x u_\zeta), \tag{43.2}$$

eq. (40.2) becomes,

$$p_{\tilde{t}} + up_\eta + rp_\zeta = -\rho c^2 \zeta_z w_{\varepsilon_\zeta}. \tag{43.3}$$

Integrating eq. (43.3) approximately, with the time increment Δt_1, and then differentiating with respect to ζ, we obtain,

$$(p^{n+1})_\zeta \simeq (p^n)_\zeta - \Delta t_1[(up_\eta + rp_\zeta)^n]_\zeta - \Delta t_1 \zeta_z(\rho c^2 w_{\varepsilon_\zeta})_\zeta. \quad (43.4)$$

where the superscripts n and n+1 denote respectively times t_n and $t_n + \Delta t_1$. With eq.(43.4), eq.(40.4) becomes,

$$\begin{aligned} \tfrac{4}{3}\mu\zeta_z^2(1 + \frac{\Delta t_1}{\Delta t_2})w_{\varepsilon_{\zeta\zeta}} &= -\tfrac{4}{3}\mu\zeta_z^2 w^*_{\zeta\zeta} - \tfrac{1}{3}\zeta_x\zeta_z\mu u_{\zeta\zeta} \\ &+ \tfrac{2}{3}\mu\zeta_z(\zeta_x)_\zeta u_\zeta + \rho(uw_\eta + rw_\zeta) - \Delta t_1\zeta_z^2(\rho c^2)_\zeta w_{\varepsilon_\zeta} \\ &+ \zeta_z[p^n - \Delta t_1(up_\eta + rp_\zeta)^n]_\zeta. \end{aligned} \quad (43.5)$$

From eqs.(39), $\frac{\Delta t_1}{\Delta t_2} = \frac{3}{4}(\frac{L}{\lambda})(\frac{1}{m})$. Assuming that the Mach Number is not large, say,

$$M < 1, \quad (44.1)$$

we conclude, from assumption (37), that

$$\frac{\Delta t_1}{\Delta t_2} >> 1. \quad (44.2)$$

It is therefore appropriate (see Section II.A) to take the quasisteady limit of eq.(42.3), which thereby becomes,

$$p \equiv p^*, \text{ or } p_\zeta \equiv 0. \quad (45.1)$$

At the same time eq.(43.5) becomes,

$$\begin{aligned} \tfrac{4}{3}\mu\zeta_z^2(1 + \frac{\Delta t_1}{\Delta t_2})w_{\varepsilon_{\zeta\zeta}} &= -\tfrac{4}{3}\mu\zeta_z^2 w^*_{\zeta\zeta} - \tfrac{1}{3}\zeta_x\zeta_z\mu u_{\zeta\zeta} \\ &+ \tfrac{2}{3}\mu\zeta_z(\zeta_x)_\zeta u_\zeta + \rho(uw_\eta + rw_\zeta) - \Delta t_1\zeta_z^2(\rho c^2)_\zeta w_{\varepsilon_\zeta} \\ &- \Delta t_1\zeta_z u_\zeta p_\eta. \end{aligned} \quad (45.2)$$

Because we have taken an additional quasisteady limit,

boundary eqs.(41) need to be reexamined in terms of (35.1) and (35.2). Eq.(40.2), at $\zeta = 0$ and $\zeta = 1$, presents some difficulty: It is assumed that the equation reflects only internal properties of the fluid at $\zeta = 0$, while at $\zeta = 1$ it gives information regarding the external flow (since it is applied at the dividing streamline between the boundary layer and the external flow). Thus, eq. (40.2) is deleted at $\zeta = 0$ but retained at $\zeta = 1$. The proposed model is then as follows:

i) At $\{0 < \zeta < 1,\ 0 \leq \eta \leq 1\}$, (46.1)

eqs.(40.3), (43.2), (45.1), (45.2).

ii) At $\{\zeta = 0,\ 0 \leq \eta \leq 1\}$, (46.2)

$$u = f_{1_t} \frac{\zeta_x}{\zeta_z},$$

$$w^* = f_{1_t} / [1 + (\frac{\zeta_x}{\zeta_z})^2],$$

$$w_\varepsilon = 0.$$

iii) At $\{\zeta = 1,\ 0 < \eta \leq 1\}$, (46.3)

$$u_\zeta = 0,$$

$$p_t = \frac{\gamma p}{c} u_t,$$

$$w_{\varepsilon_\zeta} = -\frac{1}{\rho c^2} (p_{\tilde{t}} + u p_\eta),$$

$$f_{2_t} = w + u \frac{\zeta_x}{\zeta_z},$$

iv) At $\{\zeta = 1,\ \eta = 0\}$, (46.4)

p^* specified,

$$f_{2_t} \equiv 0,$$

$$p_t = \frac{\gamma p}{c} u_t,$$

$$w_{\varepsilon_\zeta} = \frac{1}{\rho c^2} (p_{\tilde{t}} + u p_\eta).$$

Remark: The possibility of inconsistencies arising at corner points was discussed in [3]. In eqs. (46) such a difficulty occurs at $\{\zeta = 1, \eta = 0\}$: Since p^* is specified, either $u_\zeta = 0$ or $p_t = \frac{\gamma p}{c} u_t$ must be deleted. This could result in some type of "inlet adjustment" length in the solution.

Finally, it is clear, from eq. (44.2) that the $w^*_{\zeta\zeta}$ term in eq. (45.2) is negligible. In addition, under usual conditions in which incompressible models are applied, one expects the remaining terms on the right side of eq.(45.2) to be small. In any case, with the assumption,

$$|w_\varepsilon| << w^*, \tag{47}$$

w_ε becomes a purely diagnostic quantity. The resulting model in $\{p, u, w\}$ is as follows:

Eqs. (46) with $w = w^*$ and w_ε deleted. (48)

In comparing model (48) with Prandtl's boundary layer equations [9, eqs.(7.7) and (7.8)], one sees that the remaining discrepancy is in the time dependence. In eqs. (48), time dependence occurs only through boundary conditions, while in Prandtl's equations, time dependence occurs through the time derivative term in the horizontal momentum equation. In some problems, particularly those involving small perturbations in time, this difference might be significant.

Summarizing, we have derived several models for possible use in boundary layer problems:

i) Eqs. (38) are proposed for compressible flow. However, this model is still incomplete:

   a) The derivation needs to be carried out for the case of variable $\frac{t_2}{\mu}$ (assumption (11)),

   b) The effect of the forcing terms needs to be considered in eq.(38.1).

ii) Eqs.(46) and (48) are proposed for incompressible boundary layers. Solutions to these equations will be presented in the next section.

Although the above models are intended to be time-dependent, a serious question remains concerning the types of time-dependent behavior retained in quasisteady models. The following remarks address this question.

Remark 1: Quasisteady models assume that appropriate time dependence for the quasisteady variables is provided by boundary conditions. A clear example, discussed in [2], is the following: Suppose the flow is completely one-dimensional (say, in the η-direction), but a thin ζ-region is maintained. Then, eqs.(38) might still be valid, but clearly cannot by themselves provide time-dependent propagation of the flow. The important point here is that eqs.(38) are internal equations, while the boundary conditions are considered separately. Appropriate boundary conditions could be to apply the full one-dimenstional equations at, say, $\zeta = 0$; these equations would be unaffected by the internal quasisteady procedure with respect to ζ. In this regard note that eqs.(46) and (48) were derived for specific boundary conditions.

Remark 2: As a second example, consider flow in a narrow channel bounded by two parallel flat plates. Without going through all details, the quasisteady model corresponding to eqs. (48) would be as follows:

i) At the "internal" points $\{0 < \zeta < 1,\ 0 \leq \eta \leq 1\}$, the same set of equations would be used: eqs. (40.3), (43.2), (45.1), (45.2),

ii) At $\{\zeta = 0$ and $\zeta = 1,\ 0 < \eta \leq 1\}$, $u = 0$, $w = 0$, $p_{\tilde{t}} = -\rho c^2 w_\zeta$,

iii) p^* specified at the inlet line $\eta = 0$.

(Note that in this problem $f_{2_t} \equiv 0$ and the equation $p_t = \frac{\gamma p}{c} u_t$ is not appropriate).

It is not expected that the above model can predict the development of the flow, beginning with stationary flow at time zero and a time-dependent pressure input at $\eta = 0$. This can be explained by noting that two of the major assumptions are not satisfied for this problem:

a) One expects the initial propagation for this problem, at any point in the flow, to resemble a one-dimensional compression wave (following which, the vertical viscous terms dominate the flow). Thus, assumption (37) is not valid at all times.

b) Unless the region is extremely thin (say, 20 mean-free paths), assumption (28.1) will not be satisfied in the neighborhood of the moving compression wave (here we interpret L to be the width of the wave).

Remark 3: Eqs. (46) cannot predict the formation of the boundary layer resulting from impulsive motion; assumption

(28.2) would not be valid. They should, however, be applicable to some types of perturbations of an existing boundary layer. An example of such a problem will be given in Section VII.

Section VII: Solutions to the Incompressible Boundary Layer Model

In Part A we consider analytic results regarding eqs. (46), and in Part B we present some numerical solutions to several time-dependent and steady-state problems.

A) Analytic Considerations

Assuming,

i) that $w_\varepsilon \sim 0$, (49.1)

ii) that the convective terms in eq.(40.3) are negligible, (49.2)

iii) that $\frac{\gamma p}{c}=\rho c$ can be considered constant in eq. (46.3), (49.3)

eqs. (46) take the following form:

$$\mu u_{\zeta\zeta} = f^2 p_\eta, u(t,\eta,0) = u_\zeta(t,\eta,1) = 0, \tag{50.1}$$

$$w_\zeta = -fu_\eta + (f_{1_\eta} + \zeta f_\eta)u_\zeta,\ w(t,\eta,0) = 0, \tag{50.2}$$

$$p_\varepsilon = \rho_0 c_0 u^{top},\ p_\varepsilon(t,0) \text{ specified}, \tag{50.3}$$

$$f_{2_t} = w^{top} - f_{2_\eta} u^{top},\ f_2(t,0) \equiv f_2(0,\eta) \equiv f_0, \tag{50.4}$$

where $f = f_2 - f_1$, $p_\varepsilon = p(t,\eta,1) - p_0$, "top" denotes $\zeta = 1$. It has been assumed that $u \equiv 0$ at $t = 0$ and that $f_{1_t} \equiv 0$.

From eqs.(50.1) and (50.2),

$$u = -(u^{top})(\zeta^2 - 2\zeta),\ u^{top} = -\frac{f^2 p_\eta}{2\mu}, \tag{51.1}$$

$$w = (\frac{\zeta^3}{3} - \zeta^2)f(u^{top})_\eta - (\zeta^2 - 2\zeta)f_{1_\eta} u^{top} - (\frac{2\zeta^3}{3} - \zeta^2)f_\eta u^{top}. \quad (51.2)$$

From eqs.(50.3) and (51.1),

$$u^{top} = - \frac{f^2}{2\mu} \rho_0 c_0 (u^{top})_\eta,$$

or (51.3)

$$(u^{top})_\eta = - \frac{2\lambda}{f^2} u^{top}.$$

From eqs. (50.4) and (51.2),

$$f_{2_t} = - \frac{2}{3} (fu^{top})_\eta. \quad (51.4)$$

From eqs.(51.3) and (51.4),

$$f_{2_t} = - \frac{2}{3} (\frac{u^{top}}{f})(ff_\eta - 2\lambda). \quad (51.5)$$

From eqs.(51.3) and (50.3), one finds the initial conditions to be as follows:

$$u^{top}(0,\eta) = u_0^{top} e^{- 2\lambda\eta/f_0^2}.$$

$$u_0^{top} = \frac{1}{\rho_0 c_o} p_\varepsilon(t,0). \quad (52)$$

The steady-state solution must satisfy

$$(fu^{top})_\eta = 0 \quad (53.1)$$

and

$$ff_\eta = 2\lambda. \quad (53.2)$$

Note that eq.(53.1) implies the conservation of mass condition, $(\int_0^1 f\, u\, d\zeta)_\eta = 0$. From eqs.(53.2), (51.3), and (50.3) the steady-state solution is,

$$f = f_0 \sqrt{1 + \frac{4\lambda x}{f_0^2}} \quad , \tag{53.3}$$

$$u^{top} = (\frac{f_0}{f})u_0^{top}, \; u_0^{top} = \frac{1}{\rho_0 c_0} p_\varepsilon(\infty,0), \tag{53.4}$$

$$p_\varepsilon = \rho_0 c_0 u^{top} \tag{53.5}$$

$$w^{top} = (\frac{2\lambda}{f} + f_{1_\eta})u^{top} \tag{53.6}$$

One can also verify from the given solutions that assumption (49.2) is valid for small Mach number:

$$|\frac{\rho_0 u u_\eta}{p_\eta}| \leq |\frac{u^{top}}{c_0}| \quad ,$$

$$|\frac{\rho r u_\zeta}{p_\eta}| \leq |\frac{\rho w \zeta_z u_\zeta}{p_\eta}| + |\frac{\rho u \zeta_x u_\zeta}{p_\eta}|$$

$$\leq 2|\frac{u^{top}}{c_0}| + 2|\frac{u^{top}}{c_0}| \quad .$$

(The last inequality assumed that $f_{1_\eta} = 0$).

It would appear from eq.(52) that, by specifying $p_\varepsilon(0,0) = 0$, the solution could start with stationary flow and generate a boundary layer. However, because $f_0 > 0$ must be arbitrarily specified, this procedure would not seem to be reasonable.

Eq. (53.3) indicates that, as expected, the steady-state boundary layer grows as $\sqrt{x}$. Also, eq.(51.5) indicates that the rate of growth of the time-dependent boundary layer would be $\frac{2}{3}u^{top}$ (assuming $\lambda < f$).

Note in the above that the model is "consistent" in terms of mass conservation independently of eq.(50.3). Thus, as is commonly done in boundary layer problems, one could specify p_η arbitrarily and obtain solutions. However, because $\zeta = 1$ is

always a streamline, not all functions for p_η will give sensible answers. For example, p_η = constant will give u^{top} = constant and, from eq.(52.1), f = constant.

The above indicates that defining the edge of the boundary layer as a streamline is considerably different than assuming that the "outer flow" is achieved at the edge (see, for example, [9, eqs.(7.5),(7.7),(7.8)]). The use of the streamline requires, for a complete interpretation, the existence of an additional transition region from the edge of the boundary layer to the free stream conditions. On the other hand, the streamline definition avoids the inconsistency in other boundary layer models of nonzero vertical velocity at the edge of the boundary layer.

Inconsistencies at the outer edge were also discussed by Telionis and Gupta [13], where it was stated that u, p, and T should satisfy the one-dimenstional time-dependent inviscid equations at the outer edge. Thus, only one of the three variables is arbitrary. Likewise, in the quasisteady model one upper boundary condition is specified, but the other variables are calculated from quasisteady equations rather than the time-dependent inviscid equations.

B) Numerical Solutions to Eqs. (46)

The problem is that of flow over a flat plate. The initial stationary fluid was chosen with properties,

$$\rho_0 = 3.2632 \times 10^{-4} \frac{kg}{m^3} \tag{54.1}$$

$$T_0 = 260°K. \tag{54.2}$$

(These are typical atmospheric values at a height of 60 km.[14]). We then have,

$$c = c_0 = \sqrt{\gamma RT_0} = 323.24\text{m/sec}, \tag{54.3}$$

$$\mu = 2.556 \times 10^{-6}\sqrt{T(°K)} = 4.121 \times 10^{-5}\ \frac{\text{kg}}{\text{m sec}}, \tag{54.4}$$

$$\lambda = \frac{\mu_0}{\rho_0 c_0} = .3907 \times 10^{-3}\ \text{m}, \tag{54.5}$$

$$p = p_0 = \rho_0 RT_0 = 24.35\ \frac{\text{kg}}{\text{m sec}^2}, \tag{54.6}$$

As discussed in Section VI, there is an initialization problem at time zero. Our procedure was as follows:

i) An initial $f_2(\eta,0) \equiv f_{2_0}$ and an initial pressure $p(0,0) \equiv p_0 + p^*$ are specified.

ii) With the exception that the quantities f_{2_t} and f_{1_t} are maintained at zero, the remaining equations of eqs.(46) are integrated timewise until a steady-state is achieved. These values are then the initial conditions for the complete time-dependent problem, and, for small Mach number, should be in close agreement with eqs.(52).

In the first problem to be discussed we chose,

$$f_{2_0} = .02\text{m} \sim 51.2\lambda, \tag{55.1}$$

$$L = 2.5\text{m} \sim 6399\lambda, \tag{55.2}$$

$$p(0,0) - p_0 = .01 \tag{55.3}$$

$$f_1(t,\eta) \equiv 0. \tag{55.4}$$

The above lengths are consistent with the scale assumptions of

the model. The pressure value is small so that the computation will represent a low Mach number.

One expects the time step in the problem to be determined by the time-dependent partial differential equations. Upon examining eqs. (46), one sees that only one such equation remains, namely that for f_2:

$$f_{2_t} = - u f_{2_\eta} + w. \tag{56.1}$$

Eq.(56.1) is a simple first order hyperbolic partial differential equation. The time step restriction, the stability condition for the upstream differencing scheme, is,

$$\Delta t < \frac{\Delta \eta}{u} . \tag{56.2}$$

The first computation was chosen with a 5 x 13 spatial mesh, $\Delta\zeta = .25$ and $\Delta\eta = L/12$, or

$$\begin{aligned} \Delta\zeta &= .25 \\ \Delta\eta &= .2083 \\ \Delta t &= 2. \end{aligned} \tag{57}$$

(As will be seen in the results, eq.(55.3) produces a maximum u of .09482, which then accounts for the choice of Δt). The computations were then repeated with the mesh cut by a factor of 2. All results discussed below are for the finer mesh.

Figures 1-6 show results obtained for this problem. Figure 1 shows the initial p and u distribution at the top after the initialization has been completed. The pressure drops from .01 at $\eta = 0$ to .000066 at $\eta = 1$, while u drops from .09482 to .000627.

Figure 2 shows the time-dependent development of the boundary layer, assuming the above initial conditions. Figure 3 displays the boundary layer growth at two specific points. Although the precise rate of growth of the boundary layer is difficult to recover from the numerical results, Figure 4 attempts to show the rate of growth: At each point x, we plot the time at which the boundary layer achieves 90% of its final steady-state thickness. Figure 5 shows the development of the pressure field and Figure 6 shows the final steady-state horizontal velocity distribution.

The initial and final steady-state values are in good agreement with the results established in Part A, as can be seen from the following tabulation.

	Calculated	Analytic	
$u^{top}(0,2.5)$	$.6270 \times 10^{-3}$	$.7176 \times 10^{-3}$	eq.(52)
$p_\varepsilon{}^{top}(0,2.5)$	$.6613 \times 10^{-4}$	$.7569 \times 10^{-4}$	
$u^{top}(0, 1.25)$	$.7711 \times 10^{-2}$	$.8249 \times 10^{-2}$	
$p_\varepsilon{}^{top}(0,1.25)$	$.8133 \times 10^{-3}$	$.8700 \times 10^{-3}$	
$f(\infty,2.5)$	.06817	.06562	eq.(53.3)
$f(\infty,1.25)$	.04938	.04851	
$u^{top}(\infty,2.5)$	.02773	.02889	eq.(53.4)
$u^{top}(\infty,1.25)$	.03792	.03838	
$w^{top}(\infty,2.5)$	$.3659 \times 10^{-3}$	$.3440 \times 10^{-3}$	eq.(53.6)
$w^{top}(\infty,1.25)$	$.6624 \times 10^{-3}$	$.6182 \times 10^{-3}$	
$f(\infty,2.5)u^{top}(\infty,2.5)$	.001890	.001897	eq.(53.1)

Table I

The results are generally as expected. The following comments are perhaps worth noting:

i) w_ε is not displayed, but throughout $|w_\varepsilon| < 10^{-4}|w|$. Thus, eq.(43.2) is the appropriate equation for vertical velocity.

ii) In this calculation, $|w| \approx 10^{-2}|u|$. Nevertheless, because of eq.(46.3), the vertical velocity is a significant quantity.

iii) As noted earlier, it is not claimed that the above results represent the correct time development of a real boundary layer (the difficulty being in the initialization). However, the time scale, particularly as exhibited in Figure 4, seems reasonable: The time rate of growth seems to be on the order of the horizontal velocity.

iv) The input quantity f_0 is clearly related to the distance one must travel from the leading edge before the quasisteady assumptions are valid.

The accuracy of the computations was checked as follows. Since the numerical scheme is first order in the time-dependent equations, the error in the computation should be reduced by at least a factor of two if the mesh is reduced by a factor of two. Let $V(t, \eta, \zeta, h)$ represent the quantity V obtained at (t, η, ζ) with a mesh $\{\Delta t, \Delta\zeta, \Delta\eta\}$, and $V^*(t, \eta, \zeta)$ represent the correct value. Letting then $\frac{h}{2}$ represent the mesh $\{\frac{\Delta t}{2}, \frac{\Delta\zeta}{2}, \frac{\Delta\eta}{2}\}$, we can make the following two checks [2]:

$$\text{i)} \quad \Delta_2 = \left|V\left(t, \eta, \zeta, \tfrac{h}{2}\right) - V^*(t, \eta, \zeta)\right| \leq \tfrac{1}{2}\,\Delta_1 \approx \tfrac{1}{2}\left|V(t, \eta, \zeta, h) - V^*(t, \eta, \zeta)\right|, \tag{58.1}$$

$$\text{ii)}\quad \Delta_2 = \left|V(t, \eta, \zeta, \frac{h}{4}) - V(t, \eta, \zeta, \frac{h}{2})\right| \leq \frac{1}{2}\Delta_1 = \frac{1}{2}\left|V(t, \eta, \zeta, \frac{h}{2}) - V(t, \eta, \zeta, h)\right|. \tag{58.2}$$

With h representing the mesh given by eq. (57) and with V* values taken from the analytic column of Table 1, we can tabulate as follows:

V	Δ_2	Δ_1	Δ_2/Δ_1
$u^{top}(0,2.5)$	$.906 \times 10^{-4}$	1.958×10^{-4}	.463
$f(\infty, 2.5)$	.00255	.00598	.426
$f(\infty,1.25)$	.00087	.00243	.358
$u^{top}(\infty,2.5)$	.00116	.00242	.479
$u^{top}(\infty,1.25)$	.00046	.00188	.245
$w^{top}(\infty,2.5)$	.00002190	.00004708	.465

Table II

One concludes that the test defined by eq.(58.1) is satisfied.

To test eq.(58.2), a third calculation, using a mesh defined by h/4, was made. The results tabulated below, again indicate that this test is also satisfied.

V	Δ_2	Δ_1	Δ_2/Δ_1
f(100, 2.5)	.00012	.00044	.273
f(100, 1.25)	.00054	.00148	.365
u(100, 2.5)	.00072	.00145	.497
u(100, 1.25)	.00064	.00136	.471
w(100, 2.5)	$.46 \times 10^{-5}$	1.63×10^{-5}	.282
w(100, 1.25)	1.76×10^{-5}	6.98×10^{-5}	.252
p(100, 2.5)	$.76 \times 10^{-4}$	1.55×10^{-4}	.490
p(100, 1.25)	$.73 \times 10^{-4}$	1.41×10^{-4}	.518

Table III

Having achieved a steady-state solution, the model should be able to predict the time-dependent effect of subsequent perturbations of the flow field. In the next problem, the lower boundary (namely, the flat plate) is perturbed to an "angle of attack" position by the following equation:

$$f_1 = \begin{cases} \dfrac{16\eta f_1^{\max}}{(t_1-t_0)^4}(t-t_0)^2(t-t_1)^2 : \quad t_0 < t < \dfrac{t_0+t_1}{2}, \\ 0: \quad t < t_0 \text{ and } t > \dfrac{t_0+t_1}{2}. \end{cases} \tag{59}$$

Eq.(59) is such that f_1 is linear in η and achieves its maximum $f_1 = f_1^{\max}$ at $\eta = 1$ and $t = \frac{t_0+t_1}{2}$. For the sample calculation we chose,

$$f_1^{\max} = .25 = (.1)L, \tag{60.1}$$

$$t_0 = 130 \text{ sec. and } t_1 = 170 \text{ sec.} \tag{60.2}$$

With this input the plate will rotate from zero incidence at $t = 130$ sec. to 5.71^{o} at $t = 150$ sec.

Results of the above computation are shown in figures 7 and 8. At time 130 sec., the flow field is near steady-state. The plate then rotates at an average velocity of .0125 m/sec. at $\eta = 1$ during the next 20 sec. Thus the vertical velocity is comparable to the horizontal velocity during a portion of this period. Figure 7 shows that the boundary layer thickness first expands and then experiences a slow decay. The final steady-state value, $f = .0667$, occurs near $t = 270$ sec., and represents approximately a 2.8% decrease in the boundary layer thickness.

Figure 8 shows horizontal velocity. One sees an initial drop followed by a rapid overshoot, and then a gradual decay. Steady-state values are achieved more rapidly then the thickness shown in figure 7. The final value, u = .02820 represents a 2.4% increase.

The steady-state vertical velocity for this problem is on the order of 10% of the horizontal velocity, while we still have $|w_e| \sim 10^{-4}|w^*|$.

Remark: The actual "length of computation" along the physical plate increased from 2.5 m. to $\sqrt{(2.5)^2 + (.25)^2} \sim 2.5125$m.

References

1) P. Gordon, "Stability of Solutions of the Compressible Navier-Stokes Equations", J. Math. Phys., V. 18, 1977, p. 1543-1552.

2) P. Gordon, "Quasi-Steady Primitive Equations with Associated Upper Boundary Conditions", J. Math. Phys., April 1979, p. 634-658.

3) P. Gordon, "Lateral Boundary Conditions for Quasisteady Atmospheric Flows", submitted for possible publication, May 1980.

4) J. C. Maxwell, "On the Dynamical Theory of Gases", Phil. Trans. Royal Soc., London, V. 157, 1867, p. 49.

5) J. P. Brazel and E. J. Nolan, "Non-Fourier Effects in the Transmission of Heat", General Electric TIS NO. 67SD212.

6) p. Vernotte, Comp. Rendus, V. 246, 1958, p. 3154.

7) C. Truesdell, Essays in the History of Mechanics, "The Creation and Unfolding of the Concept of Stress", Springer-Verlag, New York, 1968.

8) P. Gordon, "Scaling of a System of Differential Equations", SIAM J. Appl. Math., V. 30, 1976, p. 391-401.

9) H. Schlichting, Boundary Layer Theory, McGraw-Hill Book Co., Inc., New YOrk, 1955.

10) Robert W. MacCormack, "An Efficient Explicit - Implicit - Characteristic Method for Solving the Compressible Navier-Stokes Equations", Computational Fluid Mechanics, SIAM-AMS Proceedings, V. XI, American Mathematical Society, Providence, Rhode Island, 1978.

11) R. F. Warming & Richard M. Beam, "On the Construction and Application of Implicit Factored Schemes for Conservation Laws", Computational Fluid Mechanics, SIAM-AMS Proceedings, V. XI, American Mathematical Society, Providence, Rhode Island, 1978.

12) Lagerstrom, Paco. A., Laminar Flow Theory, Section B of Theory of Laminar Flow, F. K. Moore Ed., Princeton Univ. Press, 1964.

13) D. P. Telionis & T. R. Gupta, "Compressible Oscillating Boundary Layers", AIAA Journal, V. 15, 1977, p. 974-983.

14) D. H. McIntosh & A. S. Thom, Essentials of Meteorology, Springer-Verlag, New York, 1972.

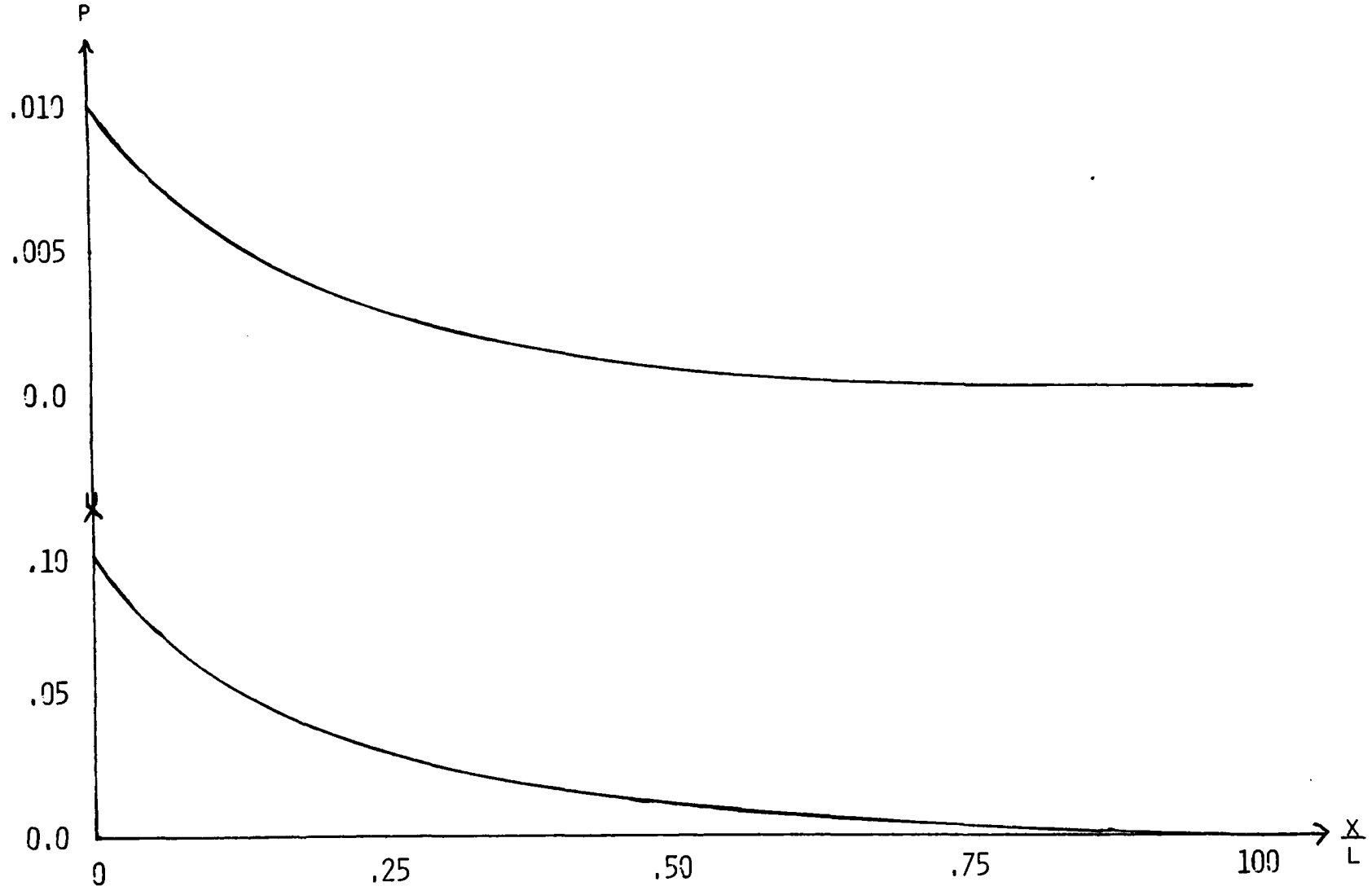

FIGURE 1: INITIAL U AND P DISTRIBUTION

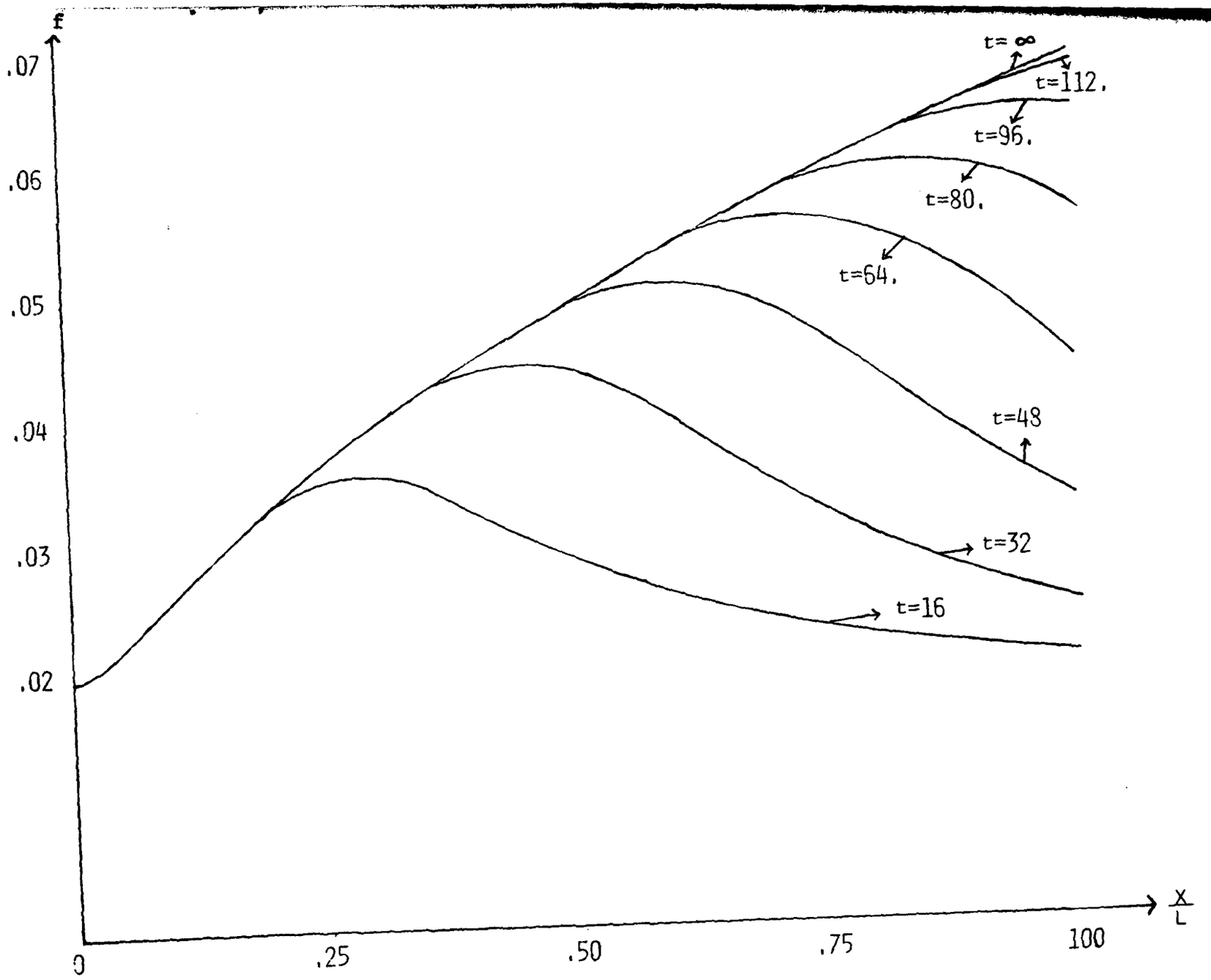

FIGURE 2: BOUNDARY LAYER GROWTH

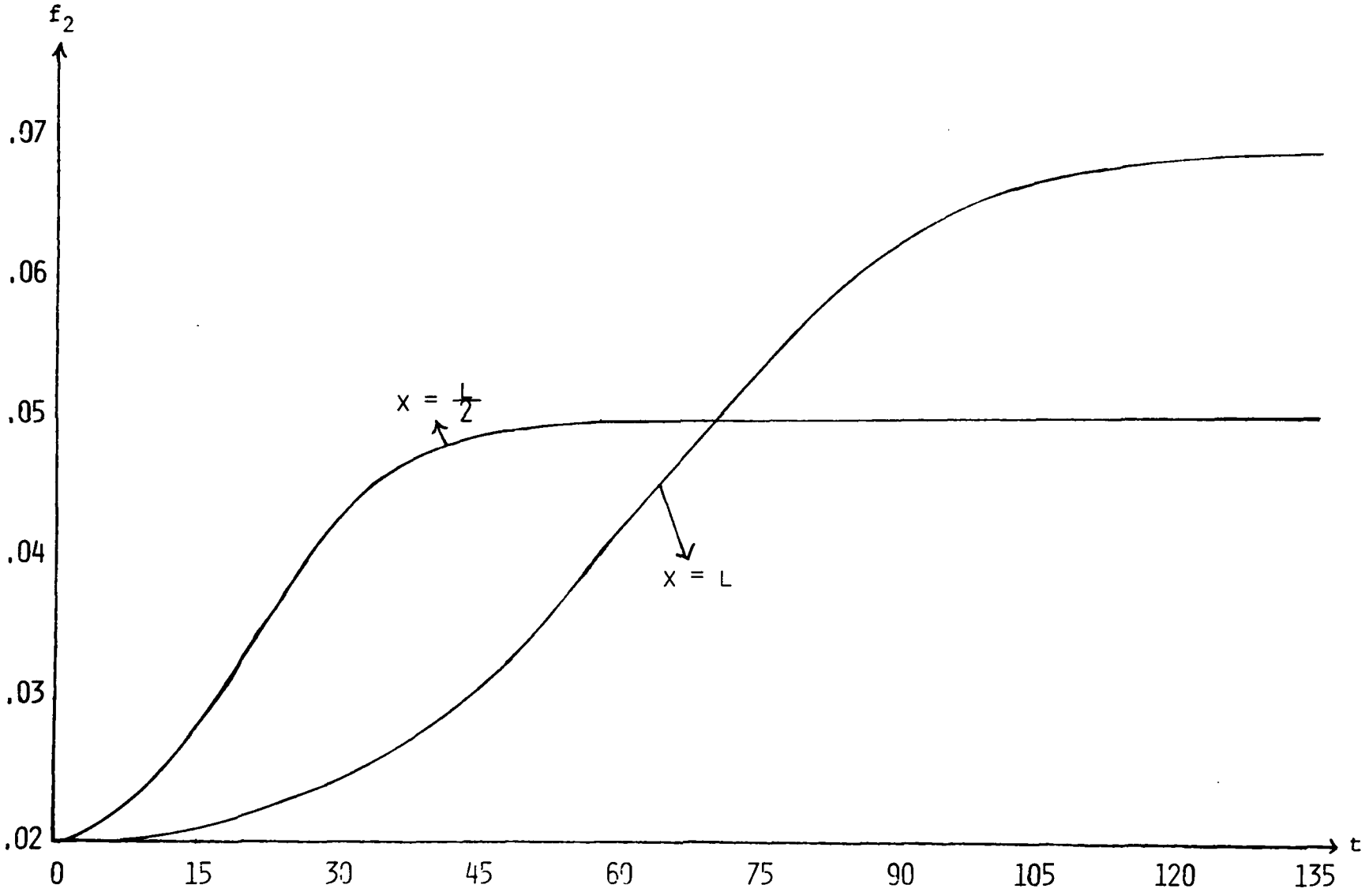

FIGURE 3: BOUNDARY LAYER GROWTH AT TWO POINTS

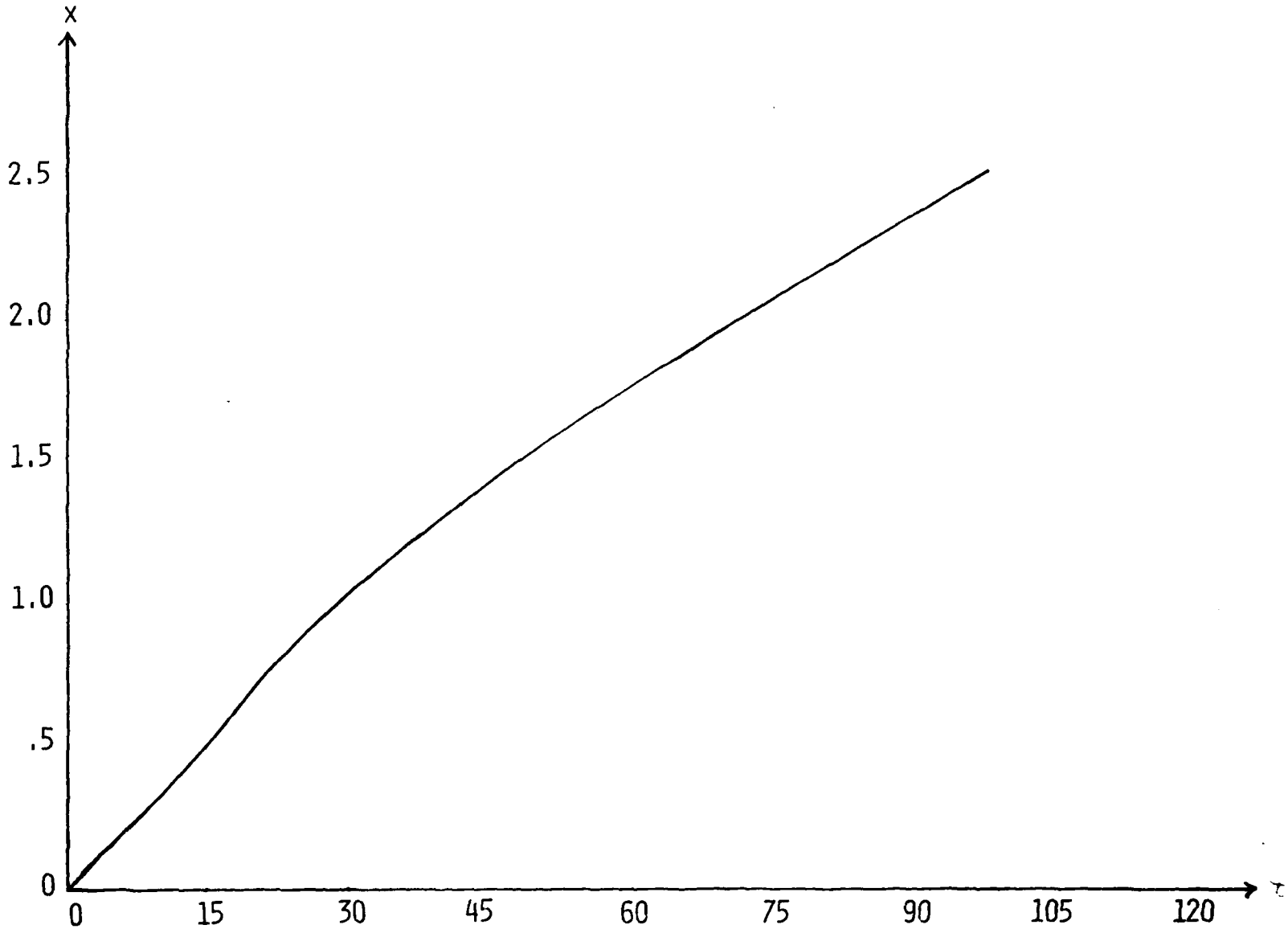

FIGURE 4: TIME AT WHICH 90% OF BOUNDARY LAYER THICKNESS ACHIEVED

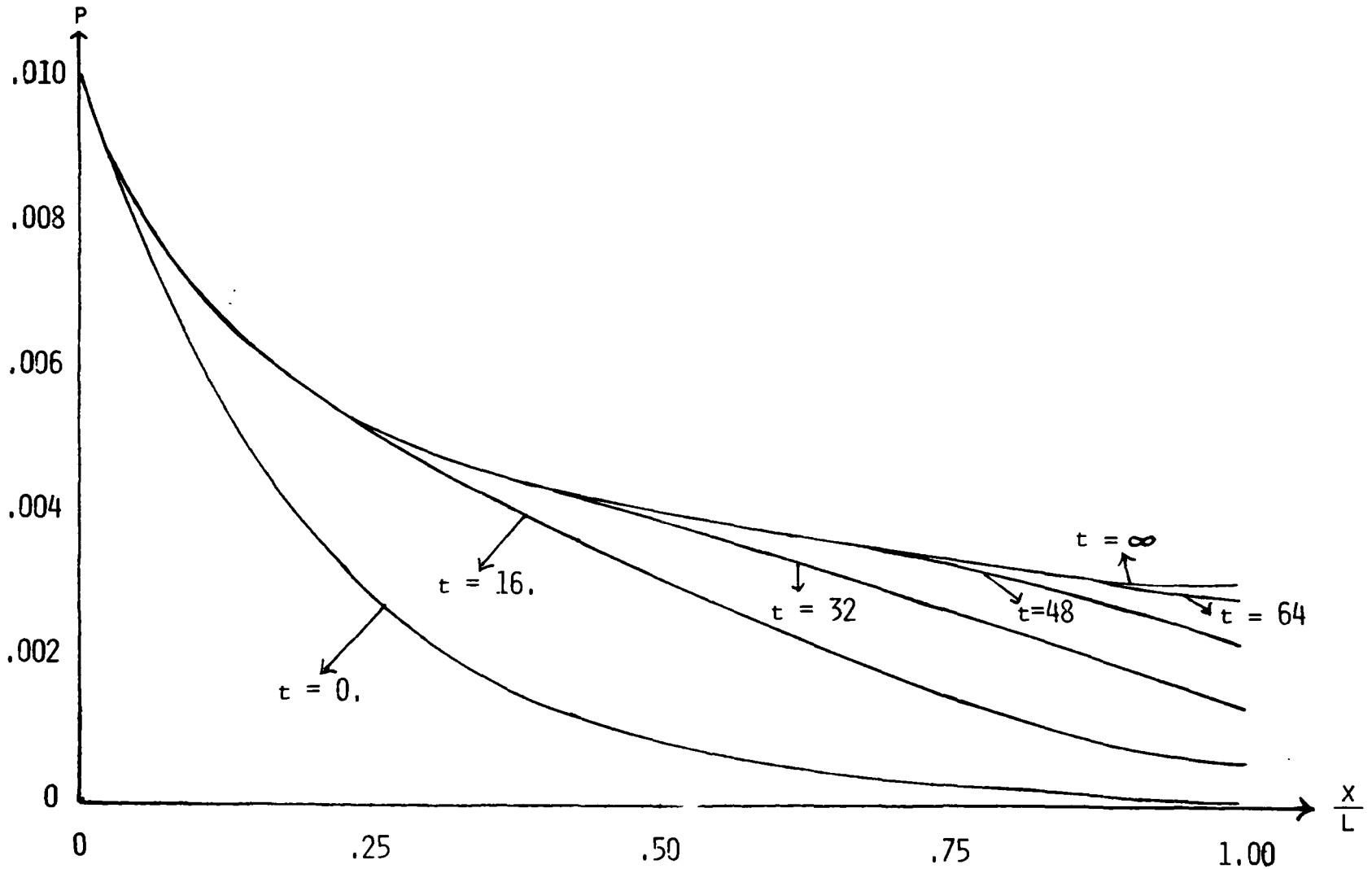

FIGURE 5: PRESSURE DISTRIBUTION

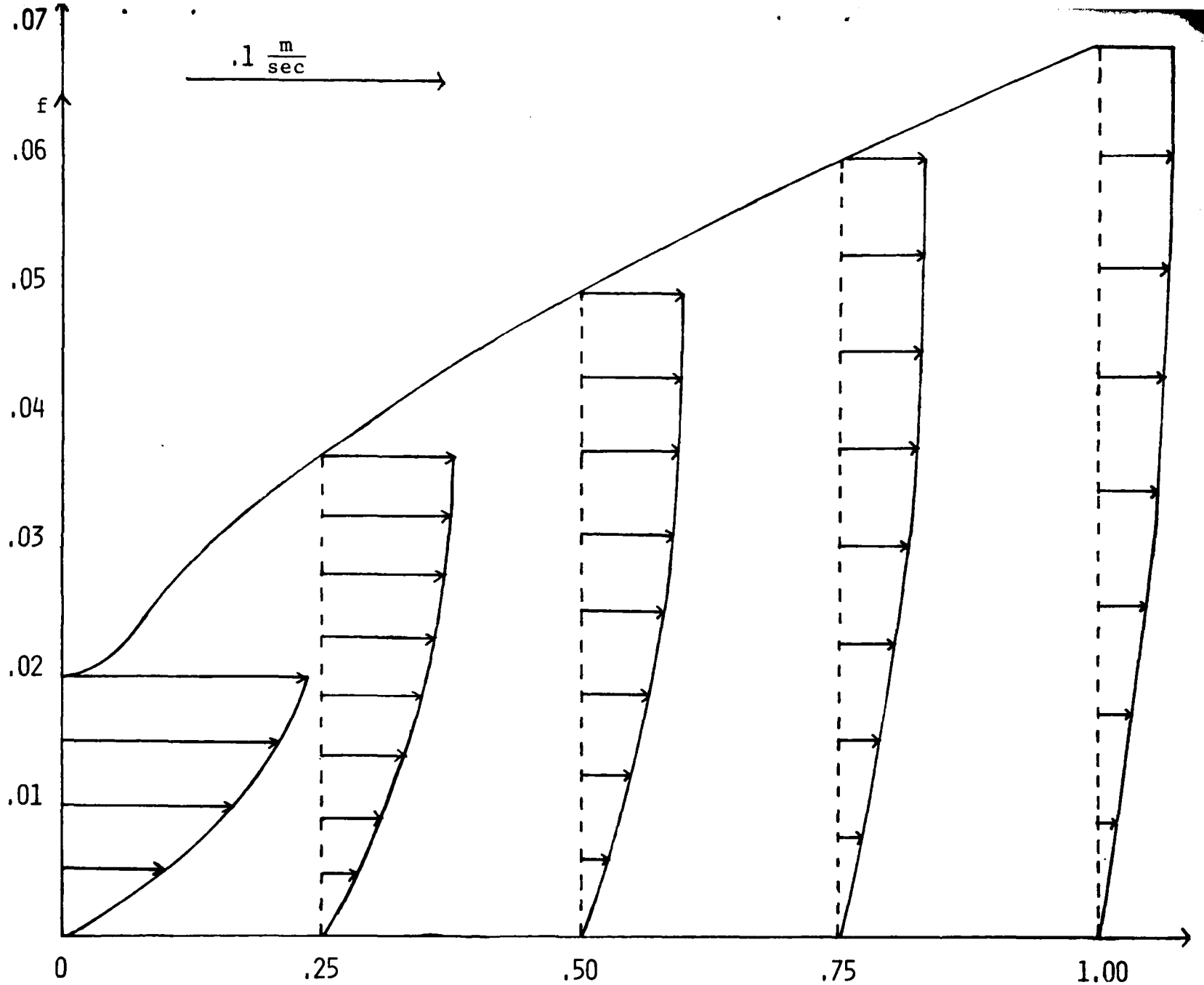

FIGURE 6: HORIZONTAL VELOCITY DISTRIBUTION

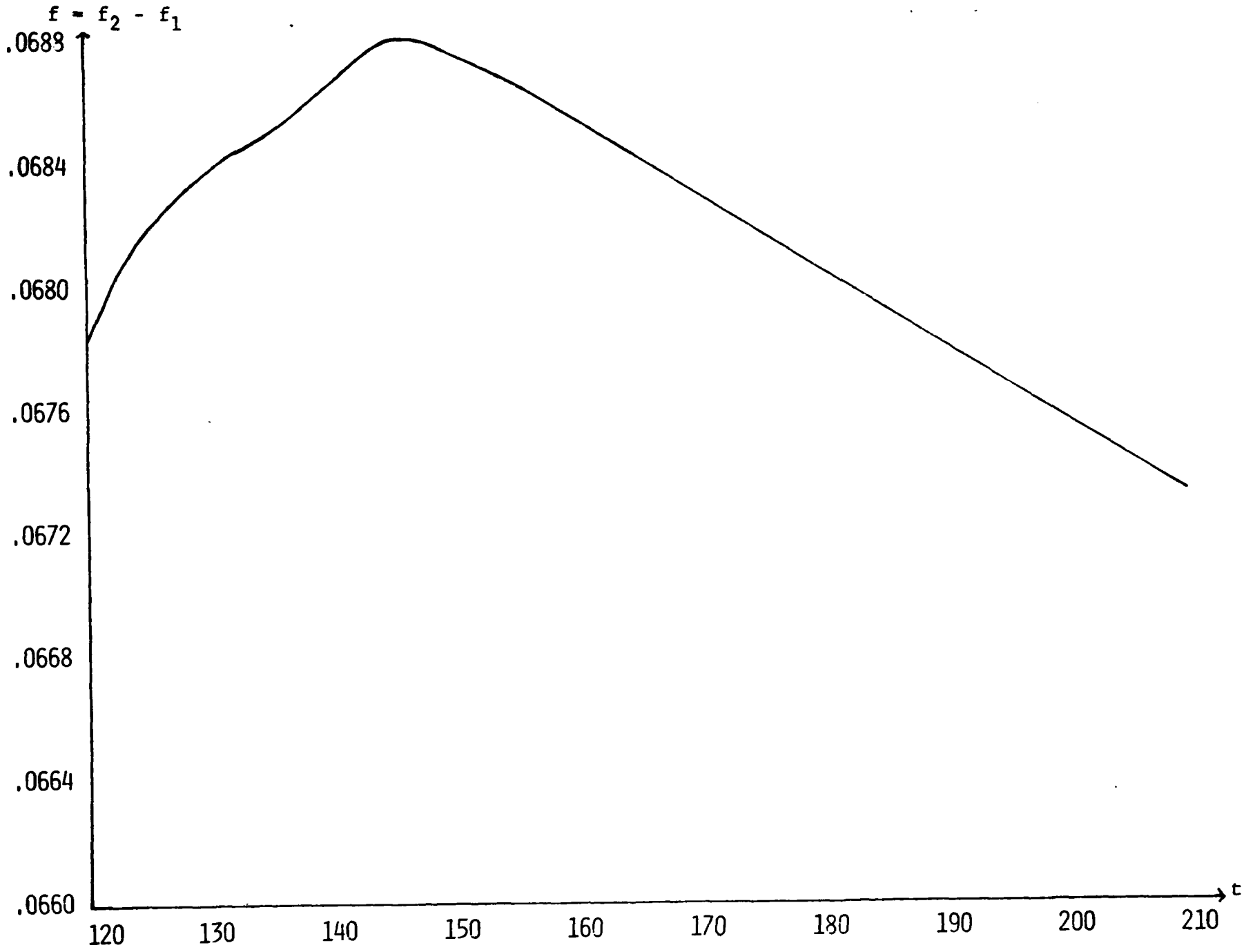

FIGURE 7: BOUNDARY LAYER THICKNESS AT NONZERO ANGLE OF INCIDENCE

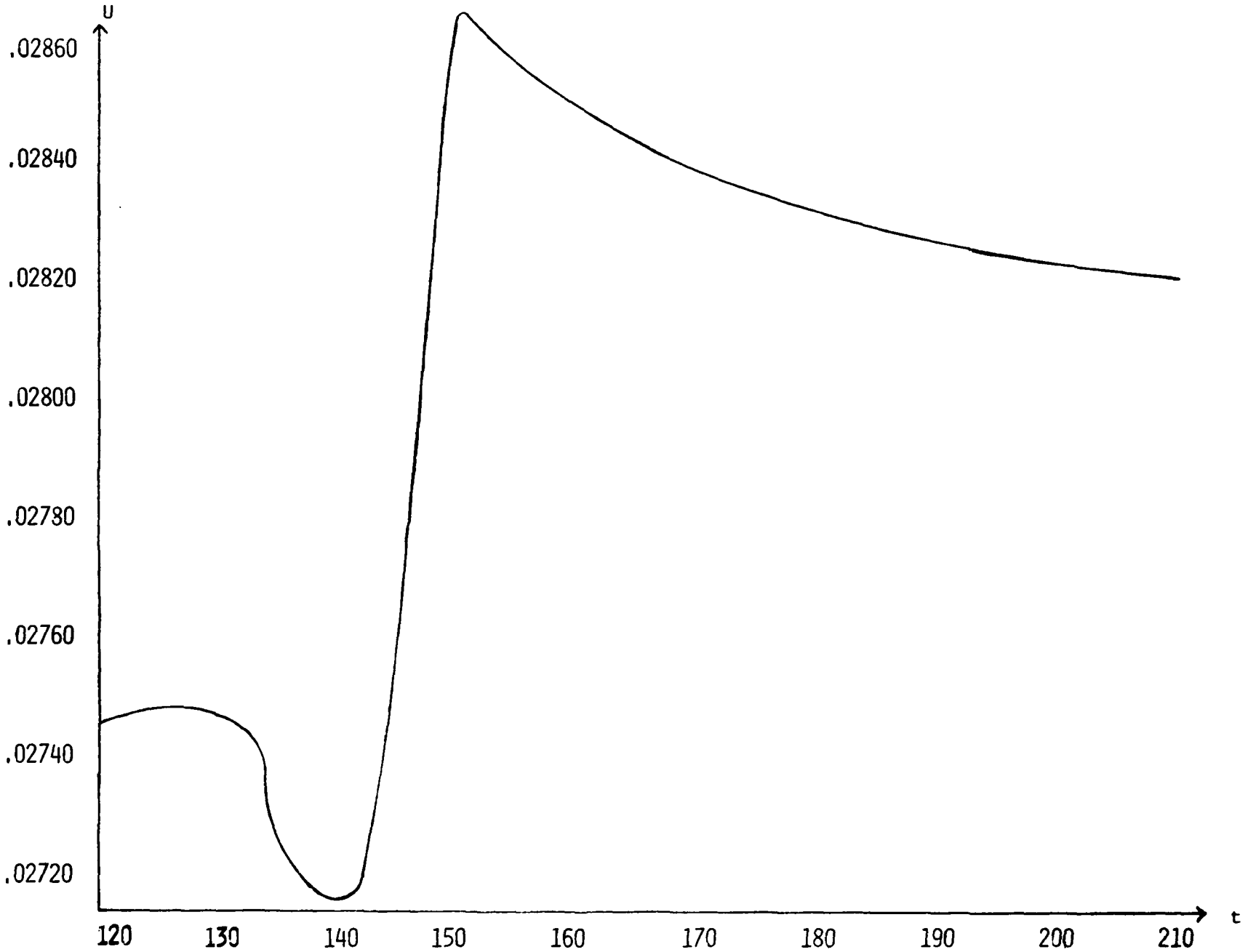

FIGURE 8: HORIZONTAL VELOCITY AFTER PLATE ROTATION AT $\eta = 1$

DISTRIBUTION LIST FOR UNCLASSIFIED
TECHNICAL REPORTS AND REPRINTS ISSUED UNDER
CONTRACT _____ TASK NR 061-254

All addresses receive one copy unless otherwise specified

Technical Library
Building 313
Ballistic Research Laboratories
Aberdeen Proving Ground, MD 21005

Dr. F. D. Bennett
External Ballistic Laboratory
Ballistic Research Laboratories
Aberdeen Proving Ground, MD 21005

Mr. C. C. Hudson
Sandia Corporation
Sandia Base
Albuquerque, NM 81115

Professor P. J. Roache
Ecodynamics Research
Associates, Inc.
P. O. Box 8172
Albuquerque, NM 87108

Dr. J. D. Shreve, Jr.
Sandia Corporation
Sandia Base
Albuquerque, NM 81115

Defense Documentation Center
Cameron Station, Building 5
Alexandria, VA 22314 12 Copies

Library
Naval Academy
Annapolis, MD 21402

Dr. G. H. Heilmeier
Director, Defense Advanced
Research Projects Agency
1400 Wilson Boulevard
Arlington, VA 22209

Mr. R. A. Moore
Deputy Director, Tactical
Technology Office
Defense Advanced Research Projects
Agency
1400 Wilson Boulevard
Arlington, VA 22209

Office of Naval Research
Code 411
Arlington, VA 22217

Office of Naval Research
Code 421
Arlington, VA 22217

Office of Naval Research
Code 438
Arlington, VA 22217

Office of Naval Research
Code 1021P (ONRL)
Arlington, VA 22217 6 Copies

Dr. J. L. Potter
Deputy Director, Technology
von Karman Gas Dynamics Facility
Arnold Air Force Station, TN 37389

Professor J. C. Wu
Georgia Institute of Technology
School of Aerospace Engineering
Atlanta, GA 30332

Library
Aerojet-General Corporation
6352 North Irwindale Avenue
Azusa, CA 91702

NASA Scientific and Technical
Information Facility
P. O. Box 8757
Baltimore/Washington International Airport
Maryland 21240

Dr. S. A. Berger
University of California
Department of Mechanical Engineering
Berkeley, CA 94720

Professor A. J. Chorin
University of California
Department of Mathematics
Berkeley, CA 94720

Professor M. Holt
University of California
Department of Mechanical Engineering
Berkeley, CA 94720

Dr. L. Talbot
University of California
Department of Mechanical Engineering
Berkeley, CA 94720

Dr. H. R. Chaplin
Code 16
David W. Taylor Naval Ship Research
and Development Center
Bethesda, MD 20084

Code 1800
David W. Taylor Naval Ship Research
and Development Center
Bethesda, MD 20084

Code 5643
David W. Taylor Naval Ship Research
and Development Center
Bethesda, MD 20084

Dr. G. R. Inger
Virginia Polytechnic Institute
and State University
Department of Aerospace Engineering
Blacksburg, VA 24061

Professor A. H. Nayfeh
Virginia Polytechnic Institute
and State University
Department of Engineering Science
and Mechanics
Blacksburg, VA 24061

Indiana University
School of Applied Mathematics
Bloomington, IN 47401

Director
Office of Naval Research Branch Office
495 Summer Street
Boston, MA 02210

Supervisor, Technical Library Section
Thiokol Chemical Corporation
Wasatch Division
Brigham City, UT 84302

Dr. G. Hall
State University of New York at Buffalo
Faculty of Engineering and
Applied Science
Fluid and Thermal Sciences Laboratory
Buffalo, NY 14214

Mr. R. J. Vidal
Calspan Corporation
Aerodynamics Research Department
P. O. Box 235
Buffalo, NY 14221

Professor R. F. Probstein
Massachusetts Institute of Technology
Department of Mechanical Engineering
Cambridge, MA 02139

Director
Office of Naval Research Branch Office
536 South Clark Street
Chicago, IL 60605

Code 753
Naval Weapons Center
China Lake, CA 93555

Mr. J. Marshall
Code 4063
Naval Weapons Center
China Lake, CA 93555

Professor R. T. Davis
University of Cincinnati
Department of Aerospace Engineering
and Applied Mechanics
Cincinnati, OH 45221

Library MS 60-3
NASA Lewis Research Center
21000 Brookpark Road
Cleveland, OH 44135

Dr. J. D. Anderson, Jr.
Chairman, Department of Aerospace
Engineering
College of Engineering
University of Maryland
College Park, MD 20742

Professor W. L. Melnik
University of Maryland
Department of Aerospace Engineering
Glenn L. Martin Institute of Technology
College Park, MD 20742

Professor O. Burggraf
Ohio State University
Department of Aeronautical and
Astronautical Engineering
1314 Kinnear Road
Columbus, OH 43212

Technical Library
Naval Surface Weapons Center
Dahlgren Laboratory
Dahlgren, VA 22448

Dr. F. Moore
Naval Surface Weapons Center
Dahlgren Laboratory
Dahlgren, VA 22448

Technical Library 2-51131
LTV Aerospace Corporation
P. O. Box 5907
Dallas, TX 75222

Library, United Aircraft Corporation
Research Laboratories
Silver Lane
East Hartford, CT 06108

Technical Library
AVCO-Everett Research Laboratory
2385 Revere Beach Parkway
Everett, MA 02149

Professor G. Moretti
Polytechnic Institute of New York
Long Island Center
Department of Aerospace Engineering
and Applied Mechanics
Route 110
Farmingdale, NY 11735

Professor S. G. Rubin
Polytechnic Institute of New York
Long Island Center
Department of Aerospace Engineering
and Applied Mechanics
Route 110
Farmingdale, NY 11735

Technical Documents Center
Army Mobility Equipment R&D Center
Building 315
Fort Belvoir, VA 22060

Dr. W. R. Briley
Scientific Research Associates, Inc.
P. O. Box 498
Glastonbury, CT 06033

Library (MS 185)
NASA Langley Research Center
Langley Station
Hampton, VA 23665

Dr. S. Nadir
Northrop Corporation
Aircraft Division
3901 West Broadway
Hawthorne, CA 90250

Professor A. Chapmann
Chairman, Mechanical Engineering
Department
William M. Rice Institute
Box 1892
Houston, TX 77001

Dr. F. Lane
KLD Associates, Inc.
7 High Street
Huntington, NY 11743

Technical Library
Naval Ordnance Station
Indian Head, MD 20640

Professor D. A. Caughey
Cornell University
Sibley School of Mechanical and
Aerospace Engineering
Ithaca, NY 14853

Professor E. L. Resler
Cornell University
Sibley School of Mechanical and
Aerospace Engineering
Ithaca, NY 14853

Professor S. F. Shen
Cornell University
Sibley School of Mechanical and
Aerospace Engineering
Ithaca, NY 14853

Library
Midwest Research Institute
425 Volker Boulevard
Kansas City, MO 64110

Dr. M. M. Hafez
Flow Research, Inc.
P. O. Box 5040
Kent, WA 98031

Dr. E. M. Murman
Flow Research, Inc.
P. O. Box 5040
Kent, WA 98031

Dr. S. A. Orszag
Cambridge Hydrodynamics, Inc.
54 Baskin Road
Lexington, MA 02173

Professor T. Cebeci
California State University. Long Beach
Mechanical Engineering Department
Long Beach, CA 90840

Mr. J. L. Hess
Douglas Aircraft Company
3855 Lakewood Boulevard
Long Beach, CA 90808

Dr. H. K. Cheng
University of Southern California,
University Park
Department of Aerospace Engineering
Los Angeles, CA 90007

Professor J. D. Cole
University of California
Mechanics and Structures Department
School of Engineering and Applied
Science
Los Angeles, CA 90024

Engineering Library
University of Southern California
Box 77929
Los Angeles, CA 90007

Dr. C. -M. Ho
University of Southern California,
University Park
Department of Aerospace Engineering
Los Angeles, CA 90007

Dr. T. D. Taylor
The Aerospace Corporation
P. O. Box 92957
Los Angeles, CA 90009

Commanding Officer
Naval Ordnance Station
Louisville, KY 40214

Mr. B. H. Little, Jr.
Lockheed-Georgia Company
Department 72-74, Zone 369
Marietta, GA 30061

Dr. C. Cook
Stanford Research Institute
Menlo Park, CA 94025

Professor E. R. G. Eckert
University of Minnesota
241 Mechanical Engineering Building
Minneapolis, MN 55455

Library
Naval Postgraduate School
Monterey, CA 93940

McGill University
Supersonic-Gas Dynamics Research
Laboratory
Department of Mechanical Engineering
Montreal 12, Quebec, Canada

Librarian
Engineering Library, 127-223
Radio Corporation of America
Morristown, NJ 07960

Dr. S. S. Stahara
Nielsen Engineering & Research, Inc.
510 Clyde Avenue
Mountain View, CA 94043

Engineering Societies Library
345 East 47th Street
New York, NY 10017

Professor A. Jameson
New York University
Courant Institute of Mathematical
Sciences
251 Mercer Street
New York, NY 10012

Professor G. Miller
New York University
Department of Applied Science
26-36 Stuyvesant Street
New York, NY 10003

Office of Naval Research
New York Area Office
715 Broadway - 5th Floor
New York, NY 10003

Dr. A. Vaglio-Laurin
New York University
Department of Applied Science
26-36 Stuyvesant Street
New York, NY 10003

Professor S. Weinbaum
Research Foundation of the City
University of New York on behalf
of the City College
1411 Broadway
New York, NY 10018

Librarian, Aeronautical Library
National Research Council
Montreal Road
Ottawa 7, Canada

Lockheed Missiles and Space Company
Technical Information Center
3251 Hanover Street
Palo Alto, CA 94304

Director
Office of Naval Research Branch Office
1030 East Green Street
Pasadena, CA 91106

California Institute of Technology
Engineering Division
Pasadena, CA 91109

Library
Jet Propulsion Laboratory
4800 Oak Grove Drive
Pasadena, CA 91103

Professor H. Liepmann
California Institute of Technology
Department of Aeronautics
Pasadena, CA 91109

Mr. L. I. Chasen, MGR-MSD Lib.
General Electric Company
Missile and Space Division
P. O. Box 8555
Philadelphia, PA 19101

Mr. P. Dodge
Airesearch Manufacturing Company
of Arizona
Division of Garrett Corporation
402 South 36th Street
Phoenix, AZ 85034

Technical Library
Naval Missile Center
Point Mugu, CA 93042

Professor S. Bogdonoff
Princeton University
Gas Dynamics Laboratory
Department of Aerospace and
Mechanical Sciences
Princeton, NJ 08540

Professor S. I. Cheng
Princeton University
Department of Aerospace and
Mechanical Sciences
Princeton, NJ 08540

Dr. J. E. Yates
Aeronautical Research Associates
of Princeton, Inc.
50 Washington Road
Princeton, NJ 08540

Professor J. H. Clarke
Brown University
Division of Engineering
Providence, RI 02912

Professor J. T. C. Liu
Brown University
Division of Engineering
Providence, RI 02912

Professor L. Sirovich
Brown University
Division of Applied Mathematics
Providence, RI 02912

Dr. P. K. Dai (R1/2178)
TRW Systems Group, Inc.
One Space Park
Redondo Beach, CA 90278

Redstone Scientific Information Center
Chief, Document Section
Army Missile Command
Redstone Arsenal, AL 35809

U.S. Army Research Office
P. O. Box 12211
Research Triangle, NC 27709

Professor M. Lessen
The University of Rochester
Department of Mechanical Engineering
River Campus Station
Rochester, NY 14627

Editor, Applied Mechanics Review
Southwest Research Institute
8500 Culebra Road
San Antonio, TX 78228

Library and Information Services
General Dynamics-CONVAIR
P. O. Box 1128
San Diego, CA 92112

Dr. R. Magnus
General Dynamics-CONVAIR
Kearny Mesa Plant
P. O. Box 80847
San Diego, CA 92138

Mr. T. Brundage
Defense Advanced Research Projects Agency
Research and Development Field Unit
APO 146, Box 271
San Francisco, CA 96246

Office of Naval Research
San Francisco Area Office
760 Market Street - Room 447
San Francisco, CA 94102

Library
The Rand Corporation
1700 Main Street
Santa Monica, CA 90401

Department Librarian
University of Washington
Department of Aeronautics and Astronautics
Seattle, WA 98105

Dr. P. E. Rubbert
Boeing Commercial Airplane Company
P. O. Box 3707
Seattle, WA 98124

Mr. R. Feldhuhn
Naval Surface Weapons Center
White Oak Laboratory
Silver Spring, MD 20910

Dr. G. Heiche
Naval Surface Weapons Center
Mathematical Analysis Branch
Silver Spring, MD 20910

Librarian
Naval Surface Weapons Center
White Oak Laboratory
Silver Spring, MD 20910

Dr. J. M. Solomon
Naval Surface Weapons Center
White Oak Laboratory
Silver Spring, MD 20910

Professor J. H. Ferziger
Stanford University
Department of Mechanical Engineering
Stanford, CA 94305

Professor K. Karamcheti
Stanford University
Department of Aeronautics and Astronautics
Stanford, CA 94305

Professor M. van Dyke
Stanford University
Department of Aeronautics and Astronautics
Stanford, CA 94305

Engineering Library
McDonnell Douglas Corporation
Department 218, Building 101
P. O. Box 516
St. Louis, MO 63166

Dr. R. J. Hakkinen
McDonnell Douglas Corporation
Department 222
P. O. Box 516
St. Louis, MO 63166

Dr. R. P. Heinisch
Honeywell, Inc.
Systems and Research Division -
Aerospace Defense Group
2345 Walnut Street
St. Paul, MN 55113

Professor R. G. Stoner
Arizona State University
Department of Physics
Tempe, AZ 85721

Dr. N. Malmuth
Rockwell International
Science Center
1049 Camino Dos Rios
P. O. Box 1085
Thousand Oaks, CA 91360

Rockwell International
Science Center
1049 Camino Dos Rios
P. O. Box 1085
Thousand Oaks, CA 91360

The Library
University of Toronto
Institute of Aerospace Studies
Toronto 5, Canada

Professor W. R. Sears
University of Arizona
Aerospace and Mechanical Engineering
Tucson, AZ 85721

Professor A. R. Seebass
University of Arizona
Department of Aerospace and
Mechanical Engineering
Tucson, AZ 85721

Dr. S. M. Yen
University of Illinois
Coordinated Science Laboratory
Urbana, IL 61801

Dr. K. T. Yen
Code 3015
Naval Air Development Center
Warminster, PA 18974

Air Force Office of Scientific
Research (SREM)
Building 1410, Bolling AFB
Washington, DC 20332

Chief of Research & Development
Office of Chief of Staff
Department of the Army
Washington, DC 20310

Library of Congress
Science and Technology Division
Washington, DC 20540

Director of Research (Code RR)
National Aeronautics and
Space Administration
600 Independence Avenue, SW
Washington, DC 20546

Library
National Bureau of Standards
Washington, DC 20234

National Science Foundation
Engineering Division
1800 G Street, NW
Washington, DC 20550

Mr. W. Koven (AIR 03E)
Naval Air Systems Command
Washington, DC 20361

Mr. R. Siewert (AIR 320D)
Naval Air Systems Command
Washington, DC 20361

Technical Library Division (AIR 604)
Naval Air Systems Command
Washington, DC 20361

Code 2627
Naval Research Laboratory
Washington, DC 20375

SEA 03512
Naval Sea Systems Command
Washington, DC 20362

SEA 09G3
Naval Sea Systems Command
Washington, DC 20362

Dr. A. L. Slafkosky
Scientific Advisor
Commandant of the Marine Corps
(Code AX)
Washington, DC 20380

Director
Weapons Systems Evaluation Group
Washington, DC 20305

Dr. P. Baronti
General Applied Science
Laboratories, Inc.
Merrick and Stewart Avenues
Westbury, NY 11590

Bell Laboratories
Whippany Road
Whippany, NJ 07981

Chief of Aerodynamics
AVCO Corporation
Missile Systems Division
201 Lowell Street
Wilmington, MA 01887

Research Library
AVCO Corporation
Missile Systems Division
201 Lowell Street
Wilmington, MA 01887

AFAPL (APRC)
AB
Wright Patterson, AFB, OH 45433

Dr. Donald J. Harney
AFFDL/FX
Wright Patterson AFB, OH 45433

DR. H YOSHIHARA
BOEING AEROSPACE COMPANY
P O. BOX 3999
MAIL STOP 41-18
SEATTLE, WA 98124